André Gonçalves Carvalho Preto

Licenciatura em Bioquímica na Faculdade de Ciências
da Universidade de Lisboa

The Role of DsrC in Dissimilatory Sulfite Reduction

Dissertação para obtenção do Grau de Mestre em
Bioquímica para a Saúde

Orientador: Dra. Inês A. C. Pereira, ITQB
Co-orientador: Dra. Sofia Venceslau, ITQB

Dezembro 2015

André Gonçalves Carvalho Preto

Licenciatura em Bioquímica na Faculdade de Ciências
da Universidade de Lisboa

The Role of DsrC in Dissimilatory Sulfite Reduction

Dissertação para obtenção do Grau de Mestre em
Bioquímica para a Saúde

Orientador: Dra. Inês A. C. Pereira, ITQB
Co-orientador: Dra. Sofia Venceslau, ITQB

Júri

Presidente: Dr. Pedro Matias, Investigador Principal do ITQB UNL
Arguente: Dr. João Bogalho Vicente, Investigador Auxiliar do ITQB UNL
Vogais: Dra. Margarida Archer, Investigadora Principal do ITQB UNL e
Dr. Inês Cardoso Pereira, Investigadora Principal do ITQB UNL

Instituto de Tecnologia Química e Biológica António Xavier

Dezembro 2015

Copyright

O Instituto de Tecnologia Química e Biológica António Xavier e a Universidade Nova de Lisboa têm o direito, perpétuo e sem limites geográficos, de arquivar e publicar esta dissertação através de exemplares impressos reproduzidos em papel ou de forma digital, ou por qualquer outro meio conhecido ou que venha a ser inventado, e de a divulgar através de repositórios científicos e de admitir a sua cópia e distribuição com objetivos educacionais ou de investigação, não comerciais, desde que seja dado credito ao autor e editor.

Acknowledgments

First of all I would like to take this opportunity to thank my supervisor Dra. Inês Cardoso Pereira for accepting me in this project and letting me work and learn in the Bacterial Energy Metabolism Lab. Her guidance, knowledge and motivation helped me a lot during this past year.

I also want to thank my co-supervisor Dr. Sofia Venceslau for teaching me all the experimental procedures presented here and the patience, attention and time she spent with me. Furthermore the freedom she offered me to plan my experiences gave me enthusiasm and confidence in my work.

I want to thank my colleagues Américo Duarte, Mónica Martins, Cláudia Mourato, Sónia Zacarias, André Santos and Irene Racagni who provided such a good environment at the work place and gave me so many good advices.

As it should be I have to thank all my friends that accompanied me through my learning process since school days till college. They are the ones that helped through the whole process and made this such a wonderful and enjoyable journey. I also have to acknowledge my colleges and friends from my master's, especially Francisca Arez, Valeria Girlus and Alina Kulakova for all those hilarious coffee breaks that turned ITQB such a good place to work in.

Finally I thank the most important people in my life, my parents and brother, for all their support, love and care. Their sacrifices both financially and emotionally throughout the years is what made this all possible and I should be eternally gratefully.

Abstract

Studies involving the human gastrointestinal microbiota and its metabolites have revealed the presence of sulfate-reducing bacteria (SRB) within the gut. These microorganisms have been implicated in inflammatory bowel diseases due to the toxic effects of sulfide, produced during dissimilatory sulfate reduction, leading to cell inflammation. The reduction of sulfite to sulfide is carried out by the dissimilatory sulfite reductase, DsrAB, and also involves the DsrC protein, which is a major protein in the cell and contains two conserved redox-active cysteines in a flexible C-terminal arm. The disulfide bond formed between these two conserved cysteines during sulfite reduction is believed to be reduced by several proteins that are related to the catalytic subunits of the heterodisulfide reductases (Hdr) of methanogens, namely HdrB and HdrD.

This work aimed to study the impact of DsrC variant strains from *Desulfovibrio vulgaris* Hildenborough in cell growth while providing ethanol or pyruvate as an electron donor and search for new physiological partners of DsrC during dissimilatory sulfate reduction in lactate-sulfate or ethanol-sulfate conditions. This work shows that a single point mutation in one of the strictly conserved cysteines (Cys93) of DsrC results in a severe decrease in cell growth indicating that DsrC, and in particular Cys93, is of major importance in the energy metabolism of these organisms. Pull down assays of DsrC coupled to mass spectrometry data and Western blot analysis showed that under ethanol-sulfate conditions DsrC interacts with the FloxABCD/HdrABC complex, ferredoxin and alcohol dehydrogenase, suggesting that these proteins are organized in a supramolecular structure. This result is in agreement with DsrC variant strains being affected under ethanol-sulfate condition and it experimentally validates a previous proposal that implicated DsrC in the ethanol oxidation pathway via the Flox/Hdr complex. Here, through DsrC, it is shown a link between the carbon metabolism and the sulfate reduction metabolism that has never been identified before.

Keywords: Inflammatory Bowel Diseases, Sulfate-reducing Bacteria, Dissimilatory sulfate reduction, DsrC, Growth Studies, Pull down assays, Mass spectrometry, Western blot

Resumo

As doenças inflamatórias intestinais (DII) são doenças crónicas que provocam a inflamação do tecido intestinal. Vários estudos realizados à flora intestinal em pacientes com DII revelaram o envolvimento de bactérias redutoras de sulfato (BRS) no desenvolvimento destas doenças devido aos efeitos tóxicos provocados pelo produto final do seu metabolismo, o sulfureto, que é produzido durante a redução dissimilativa de sulfato. A redução de sulfito a sufureto, nestes microorganismos é levada a cabo pela redutase dissimilativa de sulfito, DsrAB, e envolve uma outra proteína designada de DsrC, que possui um papel crucial dentro da célula. Esta proteína possui duas cisteínas altamente conservadas no braço fléxivel do C-terminal que durante a produção de sulfureto forma uma ligação disulfureto entre as cisteínas. Nesta forma, a DsrC encontra-se no estado oxidado e acredita-se que para voltar à sua forma reduzida, várias proteínas relacionadas com as subunidades catalíticas das reductases de heterodisulfureto de organismos metanogénicos (HdrB e HdrD) actuam como possivéis parceiros fisiológicos.

Este trabalho focou-se no estudo do impacto da DsrC no crescimento de *Desulfovibrio vulgaris* Hildenborough durante a redução dissimilativa de sulfato ou em condições fermentativas, fornecendo respectivamente etanol ou piruvato como dadores de electrões. Outro foco foi encontrar os possíveis parceiros fisiológicos da DsrC em células crescidas em meio lactato-sulfato e etanol-sulfato.

Este trabalho mostra que a mutação provocada numas das cisteínas altamente conservadas (Cys93) resulta num decréscimo acentuado no crescimento das células, o que indica que a DsrC, e em particular a Cys93, desempenha um papel crucial no metabolismo energético da célula. Os ensaios de pull down da DsrC acoplados à análise por espectrometria de massa e Western blot mostraram que a DsrC interage com o complexo FloxABCD/HdrABC e com as proteínas ferredoxina e alcoól desidrogenase na condição etanol-sulfato. Este resultado valida uma proposta já efectuada anteriormente onde a DsrC tinha sido implicada na oxidação de etanol via complexo Flox-Hdr.

Palavras-chave: Doenças inflamatórias intestinais, Bactérias redutoras de sulfato, Redução dissimilativa de sulfato, DsrC, Estudos de crescimento, Ensaios de Pull down, Espectrometria de Massa, Western blot

Table of Contents

Abbreviations List

Abs – Absorbance
Adh – Alcohol dehydrogenase
AL-DH – Aldehyde dehydrogenase
AMP – Adenosine monophosphate
AprBA – APS reductase
APC – Antigen presenting cells
APS – Adenosine 5'-phosphosulfate
ATP – Adenosine triphosphate
BCIP – 5-bromo-4-chloro-3-indolyl phosphate
CD – Crohn's disease
CoM-S-S-CoB – Heterodisulfide of CoM-SH and CoB-SH
Dsr – Dissimilatory sulfite reductase
DvH – *Desulfovibrio vulgaris* Hildenborough
$E^{0'}$ – Standard electron potential
FAD – Flavin adenine dinucleotide
Fdx – Ferredoxin
Flox – Flavin oxidoreductase
Hdr – Heterodisulfide reductase
IDB – Inflammatory Bowel Diseases
IFN-γ – Interferon- γ
IgA – Immunoglobulin A
IL – Interleukin
IMAC – Immobilized ion metal affinity chromatography
Km – Kanamycin
Ldh – Lactate dehydrogenase
MOY – MO basal medium with yeast extract
MQ – Menaquinone
MQH_2 – Menaquinol
MvhDGA – Methyl viologen-reducing hydrogenase
NAD^+ – Nicotinamide adenine dinucleotide
NADH – Nicotinamide adenine dinucleotide reduced form
NAD(P)H – Nicotinamide adenine dinucleotide phosphate
NBT – Nitro-blue tetrazolium chloride
OD – Optical density

Pi – Inorganic phosphate

PPi – Inorganic pyrophosphate

PVDF – Polyvinylidene difluoride

rRNA – ribosomal RNA

Sat – ATP sulfurylase or Sulfate adenylyltranferase

SCFA – Short chain fatty acids

SDS-PAGE – Sodium dodecyl sulfate-polyacrylamide gel electrophoresis

SRB – Sulfate-reducing bacteria

SRO – Sulfate-reducing organisms

Qmo – Quinone-interacting membrane-bound oxidoreductase

TBS – Tris-buffered saline

TGF-β – Transforming growing factor-β

Th – Helper-T-cells

TLR – Toll-like receptors

TNF-α – Tumor necrosis factor-α

Tris – Tris(hydroxymethyl)aminomethane

Treg – Regulatory T cells

UC – Ulcerative Colitis

UV – Ultraviolet

YE – Yeast extract

WT – Wild-type

Figures and Tables List

Figures

Tables

Chapter I

Introduction

1. Introduction

1.1. Sulfate-Reducing Bacteria in the Human Gut

1.1.1 Gut Microbiota

An ecological community of commensal, symbiotic and pathogenic microorganisms, inhabits the body surfaces of all vertebrates, including man. In the gut these microorganisms are very condensed and are involved in various roles such as extracting nutrients and energy from food, immune defense and in extending the metabolic repertoire of the host (1, 2, 3).

The diversity and composition of the body microbiota depends on topographical and temporal variations since the microbial community varies within each body part and are influenced by particular growth or maturation phases of the host. In humans, the microbiota composition depends not only on those but also on other factors such as diet, life-style, hygiene, antibiotic use and host's genetic disposition (Figure 1.1) (1, 4). Thus, the composition of the gut microbiota varies between individuals. All adult humans have a core microbiota which is constituted by bacteria that belong to just a few phyla. In adults, *Bacteroidetes* and *Firmicutes* usually dominate, whereas *Actinobacteria*, *Proteobacteria*, and *Verrucomicrobia* are frequent but generally minor constituents (2).

The colonization of the human gut begins after birth and by adulthood the gut presents about 10^{14} bacterial cells which is ten times the number of cells in the human body (4). The combined genomes of these microorganisms, called microbiome, provide a large variety of biochemical and metabolic activities that complement the host physiology. For example, they help the metabolism of otherwise indigestible polysaccharides and produce essential vitamins. They are also required for the development and differentiation of the human gut and confer protection against many pathogens having a crucial role in immune defense (4). Through this symbiotic relationship, the microbiota helps the development of the immune system and the latter shapes the microbe fauna in the gut. Those microbes influence the immune system through many signaling pathways that involve various classes of molecules and the resulting immune-mediated signaling processes act not only in the gut but in other organs like the brain, liver and muscle (3). The disruption of the homeostasis between the gut microbiota and the host (dysbiosis) can cause chronic inflammation and metabolic dysfunction, which ultimately can be associated with health issues like obesity, malnutrition, inflammatory bowel diseases or even cancer (2).

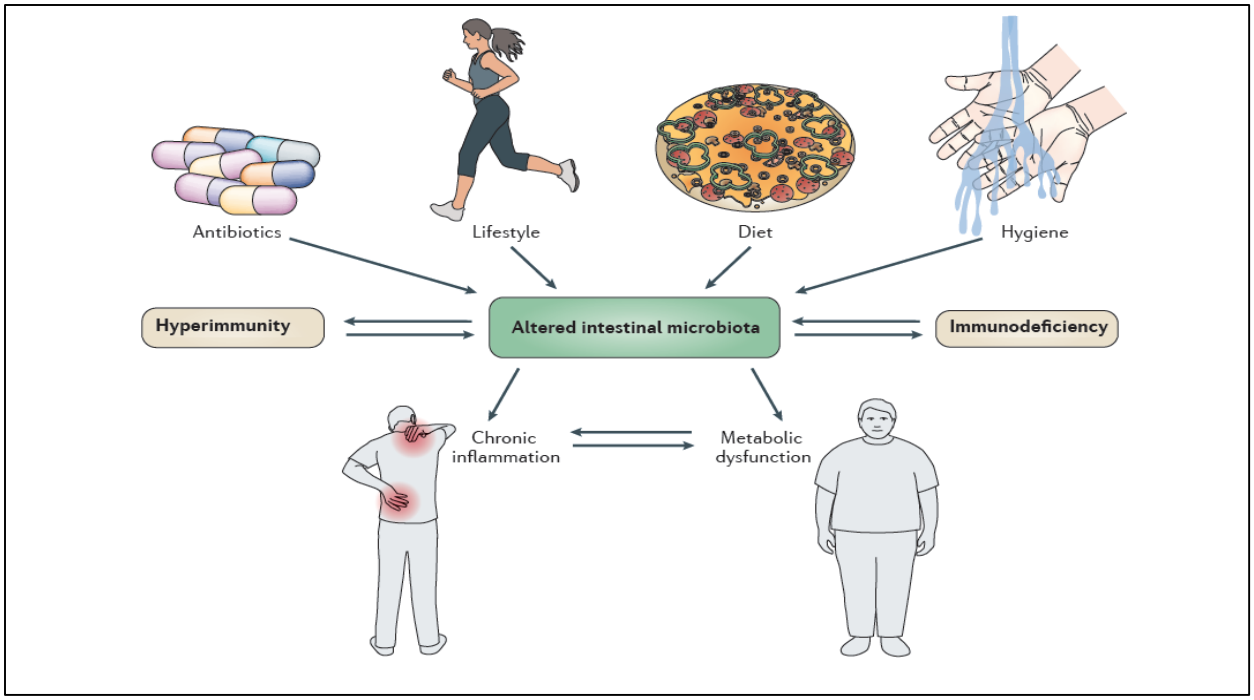

Figure 1.1 – Factors responsible for changing the gut microbiota composition and the effects of dysbiosis on hosts' health. The composition of the microbe community on the host's gut can be shaped by many factors like lifestyle, diet, hygiene or frequent use of antibiotics. In addition, the host's genetic disposition like hyperimmunity, characterized by the overexpression of pro-inflammatory mediators, or immunodeficiency, owing to mutations in regulatory immune proteins can influence that community. In turn, dysbiosis affects the levels of immune mediators and induces both chronic inflammation and metabolic dysfunction. Taken from (4).

1.1.2. Inflammatory Bowel Diseases

Inflammatory bowel diseases (IBD) are chronic inflammatory disorders that occur within the gastrointestinal tract and arise from the disruption of the immune tolerance to the gut microbiota especially in genetically predisposed hosts. The disruption is caused by a decrease in the prevalence of the major members of the human commensal microbiota (e.g. *Clostridium*, *Bacteroides* and *Bifidobacteria*) and an increase in detrimental bacteria like sulfate-reducing bacteria (SRB) (5). The detected dysbiosis is associated with the reduction of the levels of mucosal defensins, Immunoglobulin A (IgA) and malfunction of phagocytosis which weakens innate immunity and bacterial killing. Additionally, there is an overaggressive adaptive immune response to the altered gut microbiota due to increased T-cell reaction, dysfunctional regulatory T-cells (Treg) and antigen presenting cells (APC) (5).

Ulcerative colitis (UC) and Crohn's disease (CD) are considered two of the main disorders among IBD. However, they have distinct pathogenesis, inflammatory profiles and symptomatology. Both involve severe diarrhea, pain, fatigue and weight loss but inflammation linked to CD can extend deeply into submucosal regions and occurs anywhere along the gut whereas inflammation related to UC affects only the superficial layers of the intestinal mucosa and is localized into regions of the gut highly colonized by bacteria (6, 7).

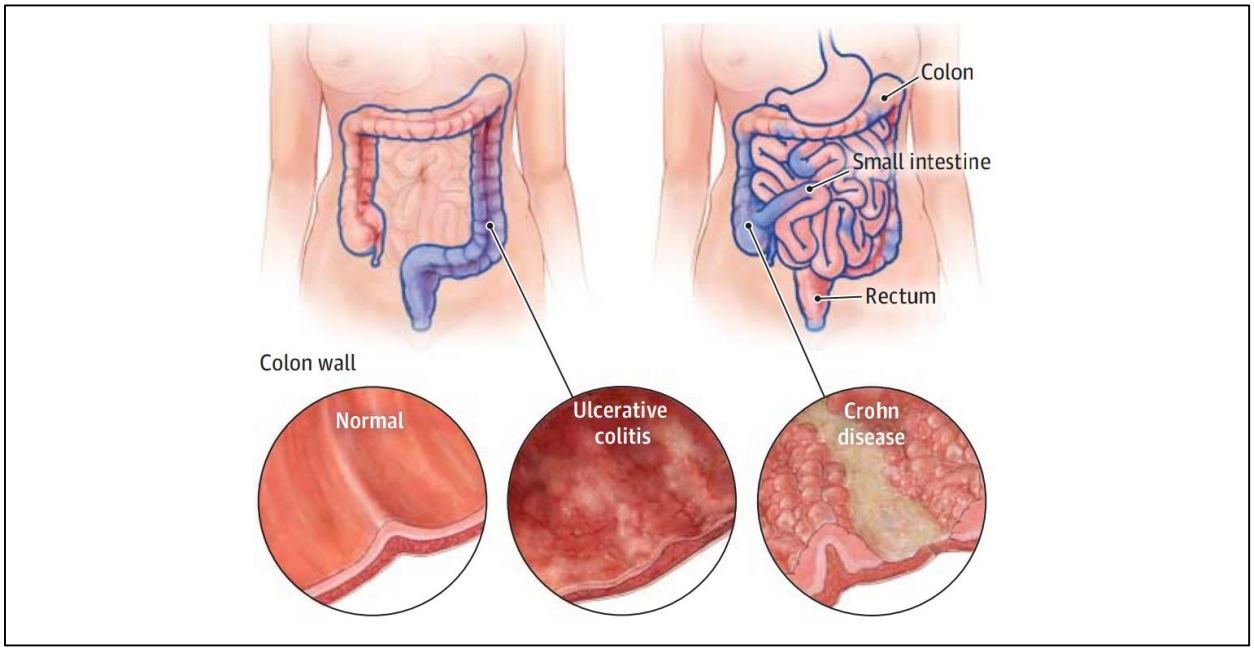

Figure 1.2 – Localization and extension of chronic inflammation induced by ulcerative colitis and Crohn's disease. Ulcerative colitis inflammation usually begins in the rectum and may extend continuously to involve the entire colon but only affects the inner layer of the bowel wall. Crohn's disease may affect any part of the gastrointestinal tract and the inflammation affects all layers of the bowel wall. Taken from (7).

The lymphocytes recruited and cytokines produced in those two diseases are also different. CD is associated with type 1 helper-T-cell (Th1) and type 17 helper-T-cell (Th17) overaggressive immune responses that increase production of interleukin (IL)-12, IL-23, IL-27, interferon-γ (IFN- γ) and tumor necrosis factor-α (TNF- α). UC seems to be associated with type 2 helper-T cell (Th2) immune responses leading to higher levels of IL-5 and transforming growth factor-β (TGF-β) (8).

1.1.3. SRB Pathogenic Role in IBD

Although not being part of the dominant members of the human gut, SRB seem to be always present in the intestinal mucosa (9, 10, 11) even though in fecal samples they are only detected in approximately 50% of healthy individuals (12). These bacteria can oxidize a wide variety of organic compounds within the large intestine like ethanol, succinate, pyruvate and lactate and are also able to use other electron donors to reduce sulfate to hydrogen sulfide (H_2S) such as volatile fatty acids (acetate, butyrate, propionate), amino acids (glutamate, alanine, serine) and indolic and phenolic compounds. Furthermore, most SRB are capable of metabolizing hydrogen resulting from bacterial fermentation (12, 13).

Distinct species of SRB belonging to the genera *Desulfovibrio*, *Desulfobacter*, *Desulfobulbus* and *Desulfotomaculum* have been identified in the human gut but the most predominant is the *Desulfovibrio* genus (10, 13) specially *Desulfovibrio piger*. The nutrients necessary for their growth are provided either

directly through the diet or from co-colonizing bacteria. For instance, *D. piger* uses sulfate directly from ingested food or indirectly from *Bacteroidetes* via sulfatases that cleave sulfated glycoproteins or even from mucopolysaccharides (long chain sugar molecules usually found in mucous surfaces of the human body) and can use hydrogen derived from fermentation (14).

Numerous studies have implicated SRB in the development of inflammatory bowel diseases especially UC and CD (5, 9, 12, 15). The hydrogen sulfide produced by these bacteria may have a pro-inflammatory action that leads genetically-susceptible individuals to develop IBD (5, 6, 11, 16). Its potential mechanism of pathogenesis is resumed in Figure 1.3.

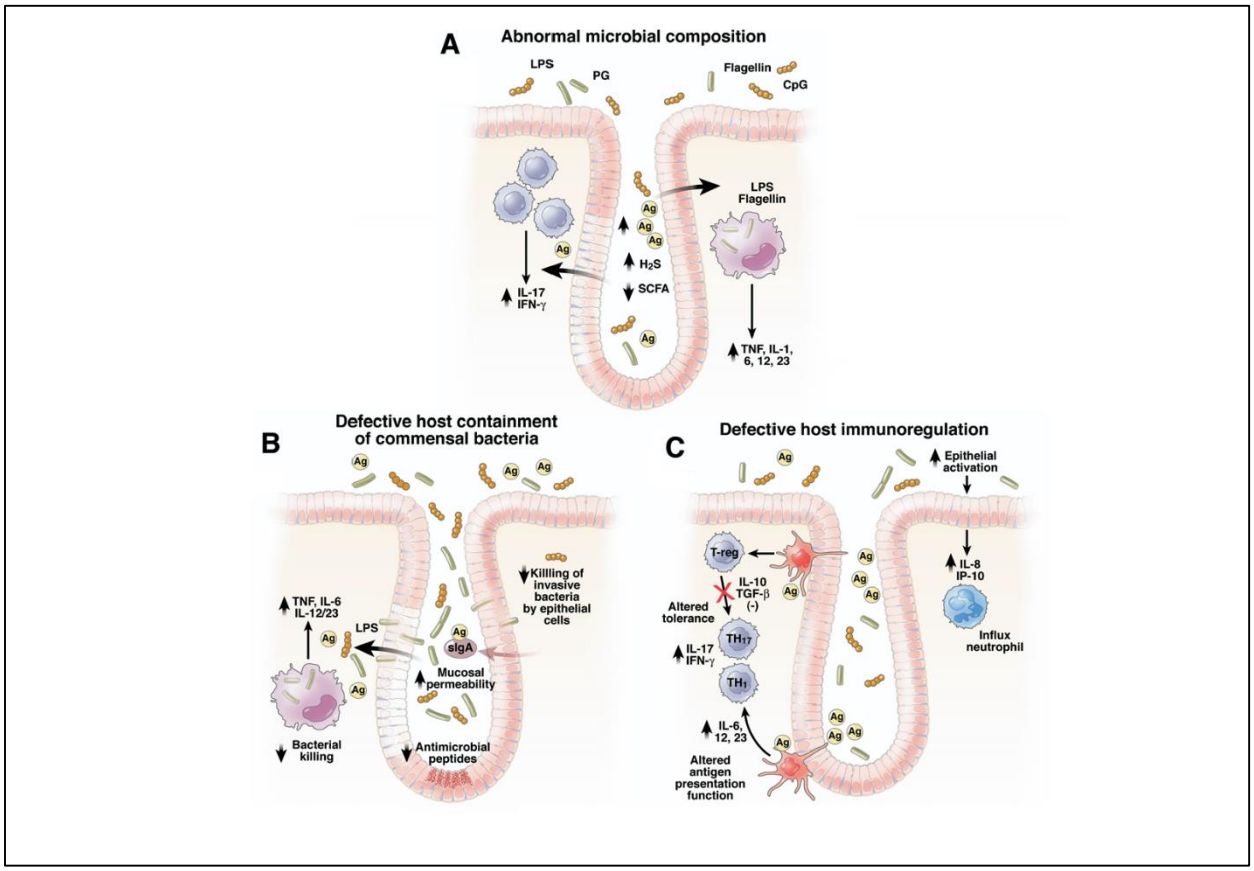

Figure 1.3 – Potential mechanism by which SRB induce chronic inflammation in IBD. (**A**) Intestinal dysbiosis in inflammatory bowel diseases is caused by decrease of putative beneficial bacteria and increase in detrimental bacteria like SRB. This imbalance causes increased levels of H_2S due to the consumption of short chain fatty acids (SCFA) like butyrate thus contributing to the down regulation of epithelial tight junction's proteins and up regulation of pore forming proteins that enhances mucosal permeability (**B**) Defective secretion of defensins or secretory IgA (also known as IgA) leads to mucosal bacterial overgrowth and increased epithelia permeability to antigens. Defective killing of phagocytosed bacteria raises intracellular bacteria concentration and consequentially increases the stimulation of bacterial toll like receptors (TLR) ligands and antigens that activate pathogenic innate and T-cell immune responses. (**C**) The disrupted mechanism of tolerance in epithelial cells and APC amplifies innate immune cell recruitment (i.e. neutrophils). Additionally, defective Treg and APC causes excessive T-cell response (Th1 and Th17), with consequential intensification of the inflammatory response and granulomatous reaction. Taken from (17).

The increased growth of SRB and decreased growth of *Clostridium* in patients with IBD can explain the reduced intraluminal levels of SFCA like butyrate. Similarly, the overgrowth of SRB can enhance the production of hydrogen sulfide blocking the use of butyrate by colonocytes (17). This contributes to the down regulation of epithelial tight junction proteins and to the upregulation of pore forming proteins thus increasing the epithelial permeability to bacteria and also a large variety of antigens (Figure 1.3 A) (18, 19). This epithelial barrier dysfunction is worsened by impaired defensin and IgA production. Defensins are antimicrobial peptides that are used to assist in killing of phagocytosed bacteria and IgA being the most secreted antibody within mucosal surfaces is responsible to entrap antigens and to down regulate epitope expression on bacterial cell surfaces and, therefore, regulate microbial intestinal colonization. Furthermore, IgA prevents attachment of pathogens, evasion of epithelial cells and removes bacteria breaching the epithelial barrier by translocating them back to the lumen and by promoting their clearance by dendritic cells, neutrophils and phagocytes (Figure 1.3 B) (20, 21). Killing of invasive bacteria that reach the lamina propria, a thin mucous layer that lies beneath gut epithelium, through the “leaky” epithelium is reduced by defective phagocytosis by macrophages. This ineffective clearance leads to the overwhelming exposure of bacterial TLR ligands and antigens that activate pathogenic innate and T-cell immune responses responsible for increasing the secretion of pro-inflammatory cytokines like TNF- α, IL-6, IL-12 and IL-23 (Figure 1.3 A and 1.3 B). The disrupted mechanism of tolerance in epithelial cells and APC amplifies innate immunity by increasing the recruitment of neutrophils. Additionally, defective Treg and APC causes activation of the nuclear factor κB (NF-κB) signaling pathway, which is usually suppressed by TGF-β and IL-10 in healthy hosts, producing overaggressive T-cell responses (Th1 and Th17) and thus intensifying the production of chemokines and pro-inflammatory cytokines such as IFN- γ and IL-17 (Figure 1.3 C) (5).

1.2. Sulfate-Reducing Bacteria (SRB)

SRB are anaerobic microorganisms that use sulfate as final electron acceptor for the degradation of organic compounds, producing sulfide in the process. It has been estimated that microbial sulfate reduction is responsible for the oxidation of 12-29% of the organic carbon flux to the sea floor, which indicates their critical role in both the sulfur and carbon cycle (22).

The study of the physiology and metabolism of SRB becomes very important not only for their implications in health but also in the environment. SRB intervene in biocorrosion of ferrous metals, as well as corrosion of concrete and stonework (23). Also, sulfide constitutes a serious problem to the petroleum industry since sulfide produced from their metabolism causes a problem called “oil souring” that affects oil fields and pipelines (23, 24, 25). The study of SRB becomes also essential for their biotechnological applications since they are able to immobilize hazardous and toxic metals released by metallurgic and nuclear plants or oil refining industry which constitutes a very useful bioremediation tool (26).

1.2.1. Sulfur Transformations

Sulfur is amongst the most abundant elements on Earth. The largest reservoirs of sulfur are iron sulfides (pyrite; FeS_2) and gypsum ($CaSO_4$) in rock and sediments, and sulfate (SO_4^{2-}) in seawater (~28 mM). The sulfur cycle is very complex since sulfur can have a wide range of oxidation states and can either be transformed chemically or biologically. The most relevant oxidation states in nature are sulfate (SO_4^{2-}; oxidation state +6), elemental sulfur (S^0; oxidation state 0), and sulfide (S^{2-}; oxidation state -2) (27).

Sulfur is taken as a nutrient by microorganisms, plants and animals that is then assimilated and incorporated in proteins and several other biological molecules, such as enzymes and vitamins. Decomposition of dead organisms in the absence of oxygen causes the release of hydrogen sulfide by desulphurylation of those molecules. Microorganisms play a very important role in all sulfur transformations (Figure 1.4).

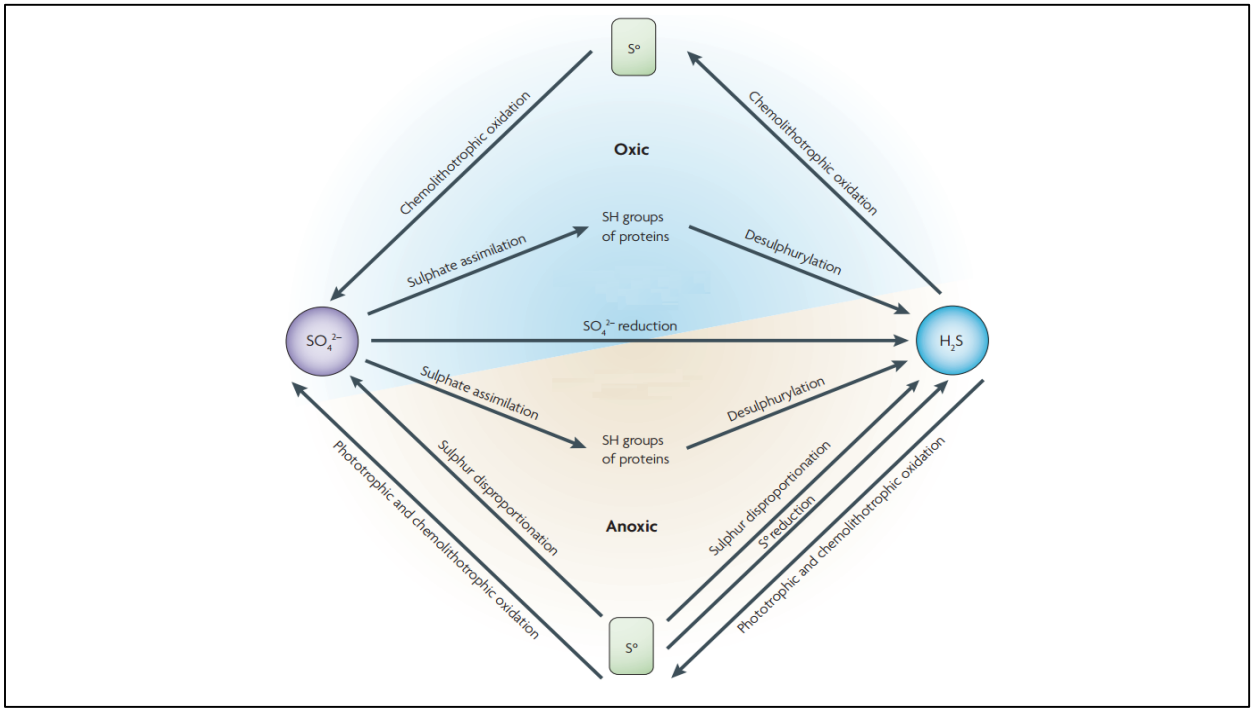

Figure 1.4 – Sulfur transformations. Sulfate (SO_4^{2-}) can either be reduced by means of assimilation to incorporate sulfur in amino acids or can be reduced by SRB through the dissimilatory sulfate reduction pathway. The sulfide (H_2S) produced in the process can be oxidized again to sulfate by chemolithotrophic and phototrophic microorganisms. Other transformations are carried out by specialized bacteria, such as elemental sulfur reduction and sulfur disproportionation. Taken from (28).

As mentioned before SRB use sulfate as a final electron acceptor to produce sulfide, which then can be oxidized to elemental sulfur and sulfate by chemolithotrophic bacteria under oxic conditions or by chemolithotrophic and phototrophic organisms under anoxic conditions. Other sulfur transformation may occur such as elemental sulfur reduction (*e.g. Desulfuromonas* spp.) and sulfur disproportionation (*e.g.*

Desulfovibrio sulfodismutans), which is a process that simultaneously produces sulfide and sulfate from elemental sulfur (28).

1.2.2. Distribution and Diversity

SRB are ubiquitous within anoxic environments such as marine sediments, fresh waters, soil and mucous surfaces of animals. They have successfully adapted to almost all ecosystems of the planet since there is evidence of their existence in high temperature and pressure environments and in a wide range of pH values (29). SRB have been identified in extremely low pH environments like acid-mine drainage sites where the pH can be as low as 2 and have been also detected in very high pH environments such as soda lakes where pH can be 10, establishing their survival capability under harsh conditions (28). Most SRB are free living, but some live in community with other microorganisms in a symbiotic way providing each other essential nutrients for their growth, such as with methanotrophic archaea and sulfate-oxidizing *Gammaproteobacteria* (30, 31).

More than 220 species of 60 genera of sulfate-reducing organisms (SRO) have been described until now (23). Based on comparative analysis of 16S ribosomal RNA (rRNA) sequences, SRO can be distributed into seven different phylogenetic lineages, five classes within the Bacteria and two classes within Archaea. Among the bacteria domain most SRB belong to the *Deltaproteobacteria* class, followed by *Clostridia*, *Nitrospirae*, *Themodesulfobacteria* and *Thermodesulfobiaceae* classes. Within Archaea SRO belong only to just a few genus of the *Euryarchaeota* and *Crenarchaeota* classes (23, 28). Almost 100 SRO already have their complete genome sequenced, e.g.*, Desulfotalea psychrophila*, *Archaeoglobus fulgidus, Desulfovibrio vulgaris* Hildenborough (DvH) and D*esulfovibrio desulfuricans G20*. The genomes of SRO belonging to the Archaea domain are usually much smaller compared to those of Bacteria. When the *Desulfotalea psychrophila* (Bacteria) and *Archaeoglobus fulgidus* (Archaea) genomes were compared small similarities were found, and these were mainly between genes for proteins involved in the dissimilatory sulfate reduction, indicating that only a small fraction of genes are necessary for sulfate reduction (32).

1.2.3. Physiology and Metabolism

Sulfate reducers are able to perform dissimilatory sulfate reduction which is an energy conservation process associated with the reduction of large amounts of sulfate necessary for their growth (23, 28, 33) and most are able to incorporate sulfide into amino acids through dissimilatory sulfite reduction (34).

SRB can use an extensive variety of electron donors and some electron acceptors, and so are metabolically versatile and can inhabit a large range of different environments. Most SRB are chemoheterotrophic organisms since they need organic carbon for cell growth and generate energy through chemical reactions. Sulfate reducers can be divided in two main groups, those who completely oxidize organic compounds to

carbon dioxide (CO_2) and those who incompletely oxidize organic compounds to acetate (Figure 1.5) (28). Regarding their electron donor metabolism, SRB can use many substrates for their growth such as monocarboxylic and dicarboxylic acids (23), sugars (35), amino acids (36), SCFA (17) and aromatic compounds (37).

Many organic macromolecules like proteins, polysaccharides and lipids cannot be directly used by SRB so they depend on other microorganisms to degrade these polymeric substrates to products that are substrates for SRB (28).

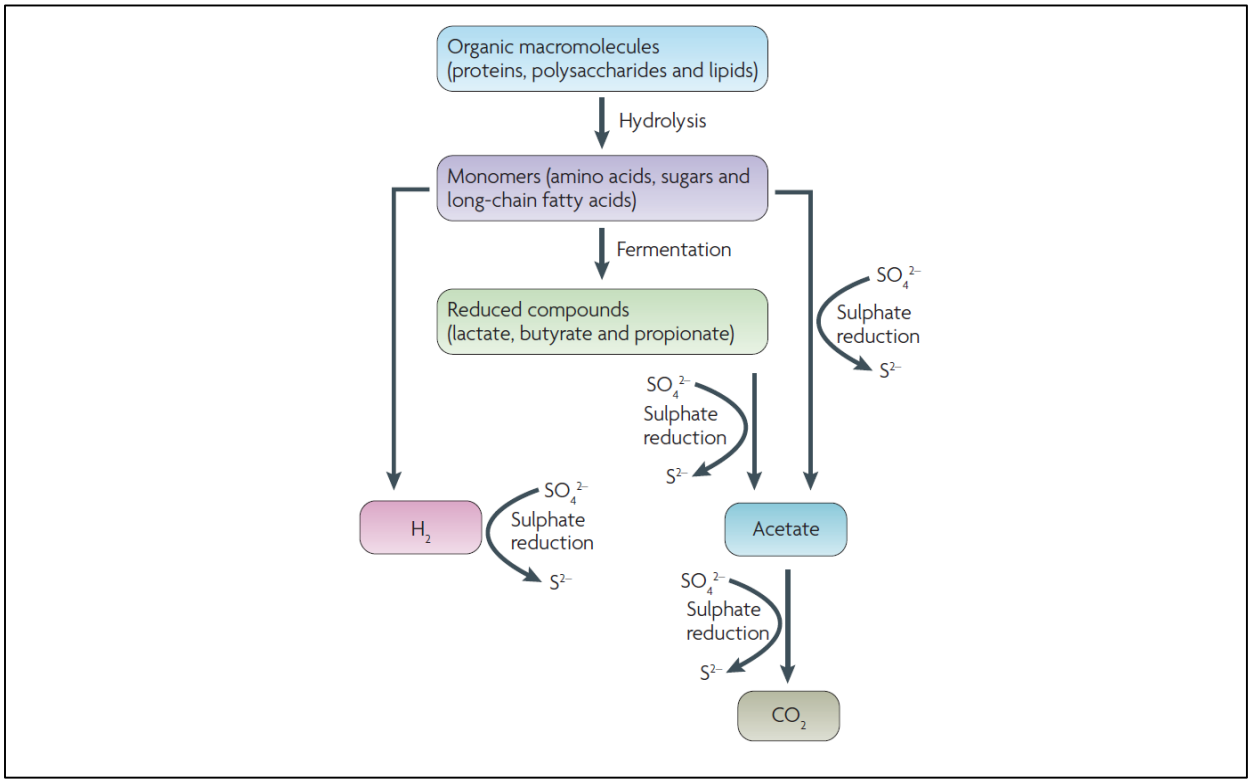

Figure 1.5 – Microbial degradation of organic matter in anoxic environments in the presence of sulfate reducers. Macromolecules like proteins, polysaccharides and lipids are hydrolyzed by hydrolytic bacteria to produce amino acids, sugars, SCFA, etc. These monomers are then fermented by fermentative bacteria into lactate, butyrate, propionate, hydrogen, acetate and other fermentative products which serve as substrates for SRB growth. Taken from (28).

Although the main electron acceptor of SRB is sulfate, other sulfur compounds such as sulfite (SO_3^{2-}), thiosulfate ($S_2O_3^{2-}$), elemental sulfur (S^0), and sulfonates can support growth of some species. Furthermore, a few species of SRB can use alternative electron acceptors like iron (Fe^{III}), uranyl (U^{VI}), selenite (Se^{VI}), chromate (Cr^{VI}), and arsenate (As^{VI}) although some of these do not contribute to cell growth (28).

1.2.4. *Desulfovibrio vulgaris* Hildenborough

According to the Integrated Microbial Genomes website there are over 60 known species of the *Desulfovibrio* genus, from which 43 genomes are available. Within the *Proteobacteria* the *Desulfovibrio* genus belongs to the *Deltaproteobacteria* class, *Desulfovibrionales* order and *Desulfovibrionaceae* family.

The most extensive biochemical and physiological studies have been done with members of the genus *Desulfovibrio,* which are the most easily and rapidly cultured sulfate reducers. The *Desulfovibrio vulgaris* Hildenborough (DvH) strain was the first SRB to have its genome sequenced (38, 39). These cells have a single polar flagellum and stain Gram negative meaning they have a cytoplasmic cell membrane (inner membrane), a thin peptidoglycan layer and an outer cell membrane with lipopolysaccharides in its outer leaflet and phospholipids in the inner leaflet. DvH uses hydrogen, alcohols or organic acids as electron donors for sulfate reduction. It uses lactate preferentially as a carbon source although other compounds can be used such as pyruvate, formate and certain primary alcohols like ethanol. The optimal growth temperature ranges from 25 to 40 ºC while the optimal pH goes from 6.6 to 7.5 (38). There is also evidence that these microorganisms are not strict anaerobes, as it was previously considered because they tolerate low levels of oxygen even though it limits growth (40).

1.3. The Dissimilatory Sulfate Reduction Pathway

The dissimilatory sulfate reduction is a process carried out by SRB that involves the eight-electron reduction of sulfate (SO_4^{2-}) to hydrogen sulfide (H_2S). This process occurs in the cytoplasm and requires the presence of sulfate transporters and three soluble enzymes - adenosine triphosphate (ATP) sulfurylase (also known as sulfate adenylyltranferase), adenosine 5'-phosphosulfate (APS) reductase and dissimilatory sulfite reductase (DsrAB/DsrC) (41). The dissimilatory reduction pathway is outlined in Figure 1.6.

First, SO_4^{2-} is transported inside the cell by symport with sodium (Na^+) or protons (H^+) (42). Due to the stability of SO_4^{2-} and its low redox potential [$E^{0'}$ (SO_4^{2-} / SO_3^{2-}) = - 526 mV], when it enters the cytoplasm, SO_4^{2-} has first to be activated by reaction with ATP to form APS, a reaction that is catalyzed by ATP sulfurylase (Sat) (Eq. 1). This endergonic reaction is driven by the hydrolysis of inorganic pyrophosphate (PPi) by a pyrophosphatase forming inorganic phosphate (Pi) (Eq. 2) (33, 42). Most of the times this reaction is carried out by soluble pyrophosphatases but in some organisms there are membrane-associated pyrophosphatases that allow proton translocation thus allowing energy conservation from hydrolysis of inorganic pyrophosphate (41).

$$SO_4^{2-} + ATP + 2H^+ \rightleftharpoons APS + PPi \qquad \Delta G^{o'} = +46\ kJ/mol \qquad (1)$$

$$PPi + H_2O \rightleftharpoons 2Pi \qquad \Delta G^{o'} = -22\ kJ/mol \qquad (2)$$

Therefore, to turn SO_4^{2-} into APS the cell needs to spend two ATP equivalents molecules, ATP and PPi. In the following step, the reduction of APS to sulfite (SO_3^{2-}) [$E^{o'}$ (APS/SO_3^{2-}) = - 60 mV] is performed by APS reductase (AprBA) and involves 2 electrons (Eq. 3) (33, 42).

$$APS + 2e^- + 2H^+ \rightleftharpoons HSO_3^- + AMP \qquad \Delta G^{o'} = -69\ kJ/mol \qquad (3)$$

The physiological electron donor for AprBA is believed to be the quinone-interacting membrane bound oxidoreductase complex (QmoABC) (43). This Qmo complex is essential for SO_4^{2-}, but not SO_3^{2-} reduction as it was confirmed in a study involving a mutant of DvH lacking the *qmoABC* genes. This mutant is incapable of growing on sulfate but can grow on sulfite or thiosulfate as electron donor (44). Finally, SO_3^{2-} is reduced by six electrons to H_2S [$E^{o'}$ (SO_3^{2-}/H_2S) = - 116 mV] (Eq. 4) via the dissimilatory sulfite reductase, DsrAB (33, 42) with the involvement of the small protein DsrC and the membrane complex DsrMKJOP (33).

$$HSO_3^- + 6e^- + 6H^+ \longrightarrow HS^- + 3H_2O \qquad \Delta G^{o'} = -172\ kJ/mol \qquad (4)$$

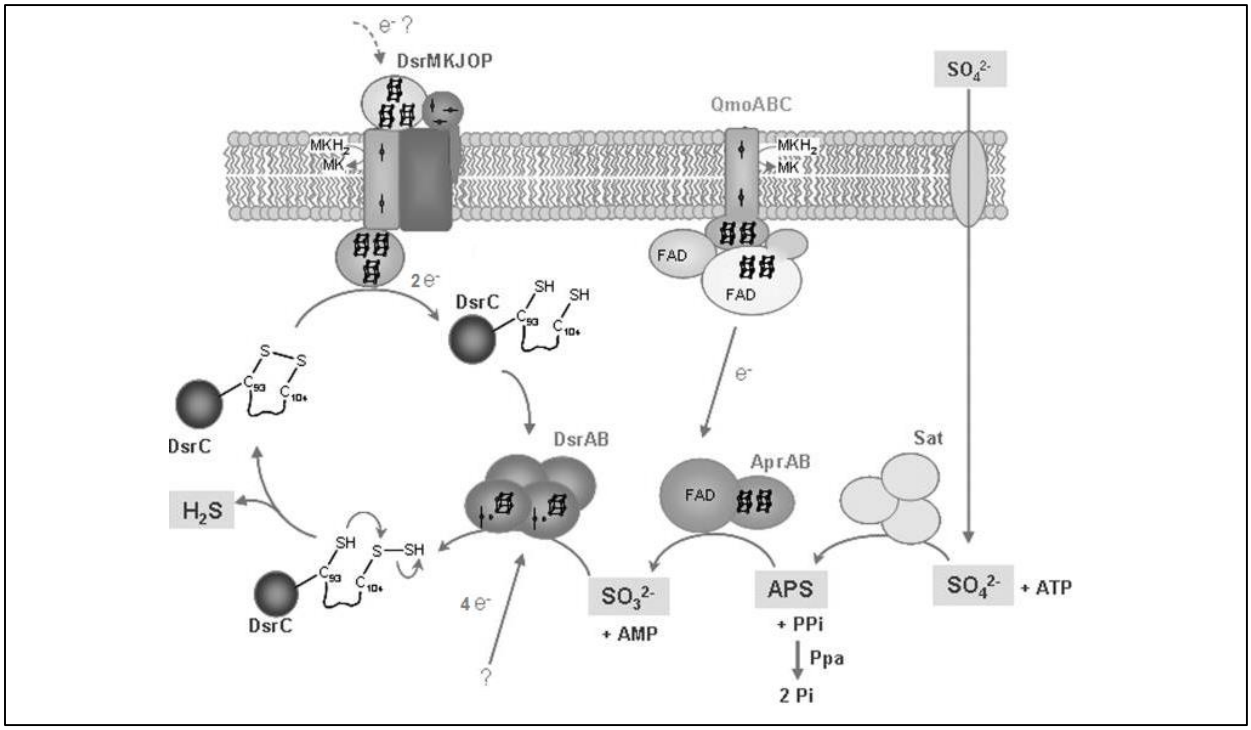

Figure 1.6 – Schematic representation of the proposed sulfate reduction mechanism. After entering the cell sulfate (SO_4^{2-}) is activated to APS by Sat. In the second step, APS receives 2 electron from the Qmo complex in a reaction catalyzed by AprBA. Finally, sulfite (SO_3^{2-}) formed in the last reaction is reduced by 6 electrons to form sulfide (H_2S) via DsrAB with the involvement of DsrC and the membrane complex DsrMKJOP. Taken from (45).

1.3.1. The DsrC protein

In SRB the dissimilatory sulfite reductase, DsrAB, is an essential enzyme that catalyzes the reduction of sulfite to sulfide. This reaction also involves a small protein of 12-14kDa named DsrC, which comprises a highly conserved C-terminal region containing two strictly conserved cysteine residues. One of these Cys is the penultimate residue of the C-terminus (C_{104} in *D. vulgaris* which was named as Cys_A) and the other one is located 10 residues upstream (C_{93} in *D. vulgaris* which was named as Cys_B) (51). DsrC was first reported as being a subunit of DsrAB in a $\alpha_2\beta_2\gamma_2$ composition. However, the *dsrC* gene is not in the same transcriptional unit as the *dsrAB* genes (46) and recently it was reported that the majority of DsrC in cell extracts of *D. vulgaris* was not associated with DsrAB, suggesting that DsrC is an interacting partner of DsrAB, and possibly of other proteins (47). DsrC is suggested to have an important role in cellular metabolism since *dsrC* is a highly expressed gene in *D. vulgaris* at the same or higher levels when compared to other proteins involved in sulfate reduction (48, 49, 50). Several 3D structures of DsrC have been determined (including *D. vulgaris*) and all present a globular shape with the exception of the C-terminal arm which adopts an extended and disordered configuration in solution but a retracted configuration in the crystal structure (45). The globular part of DsrC presents a helix-turn-helix (HTH) structural motif which is be responsible for protein binding to DNA and protein-protein interactions (Figure 1.7) (51).

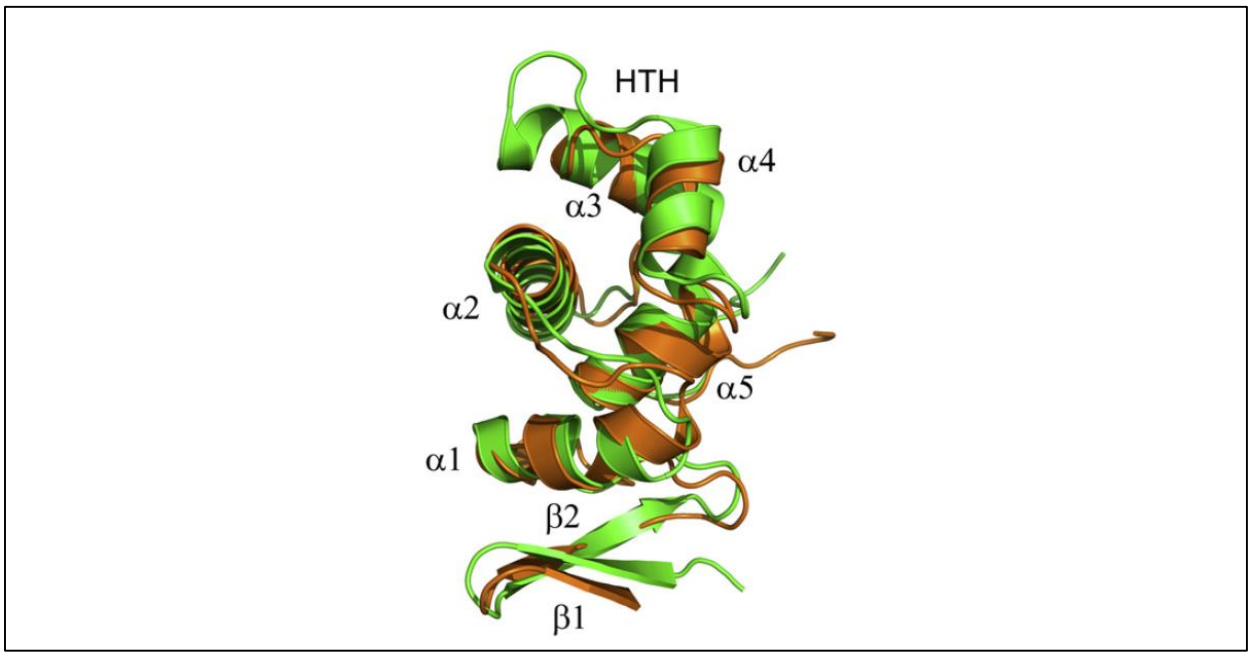

Figure 1.7 – Three dimensional structure of DsrC. Overlapping representation of DsrC from the sulfur oxidizer *Allochromatium vinosum* (green) and *D. vulgaris* (brown). DsrC presents a globular shape composed by five α–helixes, three β-sheets and a HTH structural motif. Taken from (51).

The reaction mechanism of DsrAB has been studied for many years because, in contrast to the assimilatory sulfate reduction where sulfite is directly reduced to sulfide, in dissimilatory sulfite reduction DsrAB produces *in vitro* a combination of products, mainly trithionate ($S_3O_6^{2-}$) and thiosulfate ($S_2O_3^{2-}$) (52). This led to believe that the reduction of sulfite to sulfide was dependent on the formation of trithionate and thiosulfate as intermediates. However, this suggestion was also disputed since these products of DsrAB are highly dependent on the reaction conditions which don't correspond to the ones presented *in vivo* (53). A major step to understand this mechanism was achieved when the crystal structure of this enzyme was determined. It was shown that only one catalytic siroheme-[4Fe-4S] cofactor is present per αβ unit, bound to DsrB, whereas the equivalent cofactor bound to DsrA, sirohydrochlorin (siroheme without iron) seems to have a structural role (45). Additionally through the crystal structure of DsrAB of *D. vulgaris* it was revealed that this enzyme is present in a $\alpha_2\beta_2\gamma_2$ composition with DsrC (Figure 1.8 A). It was also shown that the C-terminal of DsrC projects inside DsrAB bringing the Cys_A residue near the catalytic site where the sulfite molecule is located (Figure 1.8 B) (45).

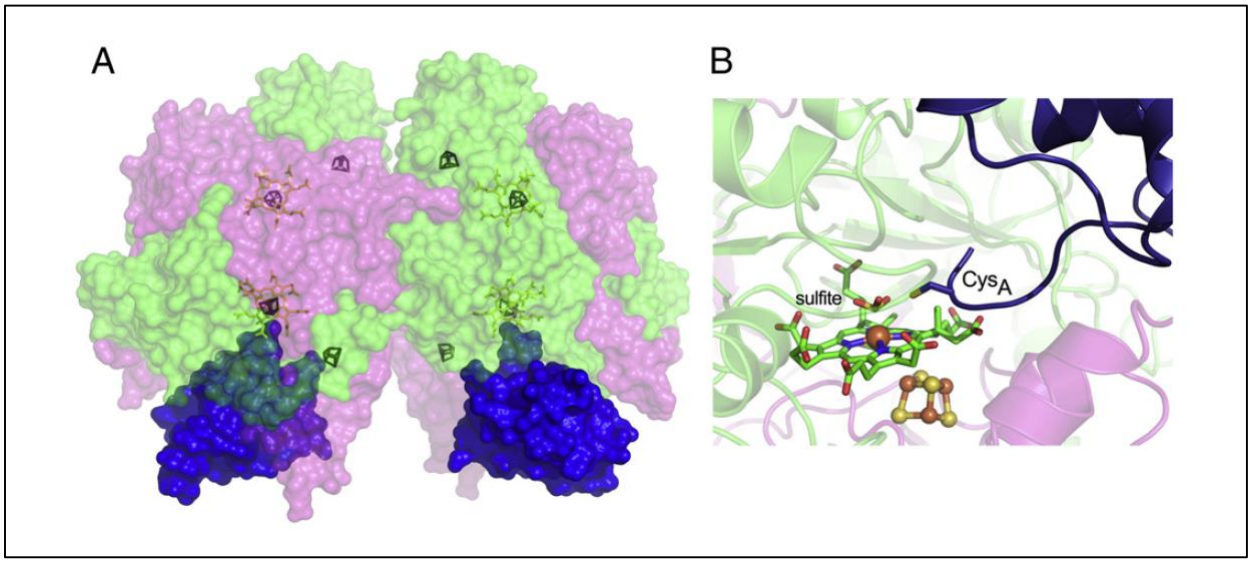

Figure 1.8 – Structure of DsrAB in complex with DsrC. (**A**) Molecular surface representation of DsrAB in a $\alpha_2\beta_2\gamma_2$ composition with DsrC. (**B**) Detailed image of the *Desulfovibrio gigas* catalytic site where it can be seen the C-terminal arm reaching for the siroheme-[4Fe-4S] active site. DrsA – green, DsrB – pink, DsrC – blue. Taken from (51).

The crystal structure of these enzymes led to the proposal of a mechanism for sulfite reduction (Figure 1.9). Sulfite is reduced by 4 electrons forming two intermediates in a S^{II} and S^0 valence state that stay bound to the DsrAB catalytic site. The S^0 intermediate then binds to DsrC Cys_A producing a persulfide as a key intermediate. This persufide upon reacting with the other conserved cysteine (Cys_B) forms a disulfide bond in DsrC (which is now in the oxidized form) and releases sulfide (45). This disulfide bond formed between the two conserved cysteines of DsrC is believed to be reduced by several proteins present in these organisms that are related to heterodisulfide reductases (Hdr) of methanogens, mainly HdrB and HdrD.

The putative physiological partners of DsrC belong to the CCG protein family, known to have a conserved cysteine-rich sequence (CX_nCCGX_mCXXC) (51). This motif binds a $[4Fe\text{-}4S]^{3+}$ cluster, which in Hdr is the catalytic cofactor responsible for the reduction of the heterodisulfide, CoM-S-S-CoB formed in the last step of methanogenesis (54). The heterodisulfide is not present in SRB, so this lead to the proposal that the disulfide bond of DsrC after the release of sulfide during sulfite reduction, can be the equivalent of the heterodisulfide in SRB. This oxidized form of DsrC can work as a substrate for proteins related to HdrB and HdrD (51).

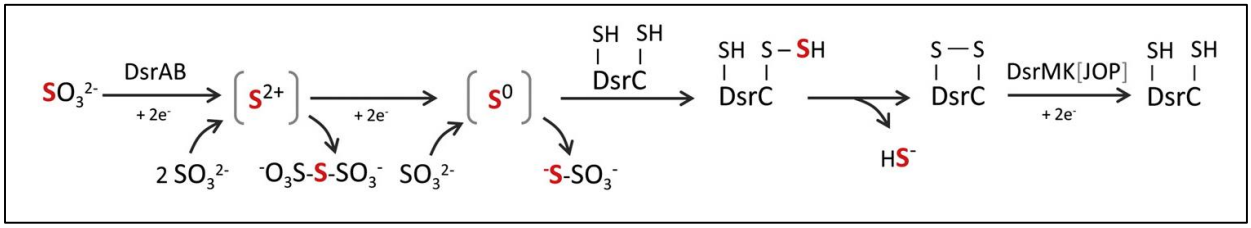

Figure 1.9 – Proposed mechanism of sulfite reduction by DsrAB and DsrC. Upon receiving 4 electrons sulfite is reduced to a S^0 valence state. This intermediate still bound to DsrAB catalytic site then reacts with Cys_A forming a persulfide. Internal reaction of this persulfide with the other cysteine forms a disulfide bond and releases sulfide. The S^{II} and S^0 intermediates can react with excess sulfide to form trithionate and thiosulfate, respectively. DsrMKJOP and maybe other HdrB/HdrD related proteins are responsible to restore the oxidized DsrC into its reduced form. Taken from (51).

The possible disulfide reductases of DsrC are presented in Figure 1.10 and include the membrane complexes DsrMKJOP, HmcABCDEF and TmcABCD that are involved in electron transfer with the periplasm and/or menaquinone (MQ) pool, and also soluble proteins involved in oxidation of several substrates, such as lactate (lactate dehydrogenase, Ldh), ethanol [alcohol dehydrogenase (Adh), flavin oxidoreductase (FloxABCD) and HdrABC] and H_2 [methyl viologen-reducing hydrogenase (MvhDGA) and HdrABC) (51).

DsrMKJOP is a transmembrane complex composed by two modules, DsrJOP that is facing the periplasm and DsrMK facing the cytoplasm (41). The DsrMK module of this complex has a CCG motif in the DsrK subunit analogous to the one found in HrdD, thus suggesting that it can reduce the oxidized form of DsrC. This can have an important role in the sulfite reduction pathway since the Dsr complex can possibly mediate electron transfer between the menaquinol (MQH_2) pool to the oxidized form of DsrC, contributing to energy conservation. The DsrJOP module is most likely involved in electron flow between the periplasm and the MQ pool, although the mechanism behind this process is not fully understood yet (55). Furthermore, there is evidence that DsrK interacts with DsrC both in *A. vinosum* (56) and *D. desulfuricans* and in the majority of SRO the genes that encode this protein complex are usually clustered with *dsrAB* and *dsrC* genes, suggesting their physiological interaction (51).

HmcABCDEF and TmcABCD are both transmembrane complexes with a cytoplasmic subunit belonging to the CCG protein family (51). In the Hmc complex the CCG motif analogous to that present in HdrD/DsrK is

found in the HmcF subunit and in the Tmc complex it is present in the TmcB subunit (41). Since these complexes have a similar architecture to DsrMKJOP and both have a subunit belonging to the CCG protein family this suggests that they might be alternative electron donors to the oxidized form of DsrC (51).

Besides the HdrD-like proteins associated with membrane complexes, there are many other Hdr-related proteins belonging to the CCG protein family that might act as electron donors to DsrC in SRB. Some of these proteins are the soluble complexes FloxABCD/HdrABC and MvhDGA/HdrABC both containing the HdrB subunit with the CCG motif. In SRB the *hdrABC genes* are found within two different sets of genes clusters: *hdrABC/floxABCD* and *hdrABC/mvhDGA* (41). The *floxABCD* genes are found in many SRB and code for a NAD(P)H (nicotinamide adenine dinucleotide phosphate) oxidoreductase that oxidizes NAD(P)H formed during ethanol oxidation by an alcohol dehydrogenase to transfer electrons to HdrABC and ferredoxin (Fdx) (57, 58). The HdrABC/MvhDGA is a complex characteristic of methanogens and present in few SRO (41). It is involved in the oxidation of H_2 by reduction of Fdx (54). These two complexes (FloxABCD/HdrABC and MvhDGA/HdrABC) are involved in a flavin-based electron bifurcation mechanism where the oxidation of ethanol and H_2, respectively, is used to reduce both Fdx and a heterodisulfide, which in SRO is proposed to be the oxidized form of DsrC (58). The link between FloxABCD and DsrC is further supported by the fact that the genes that encode these proteins are found next to each other in some organism (e.g. *Desulfobacterium autotrophicum, Desulfosarcina* sp. BuSS) (51).

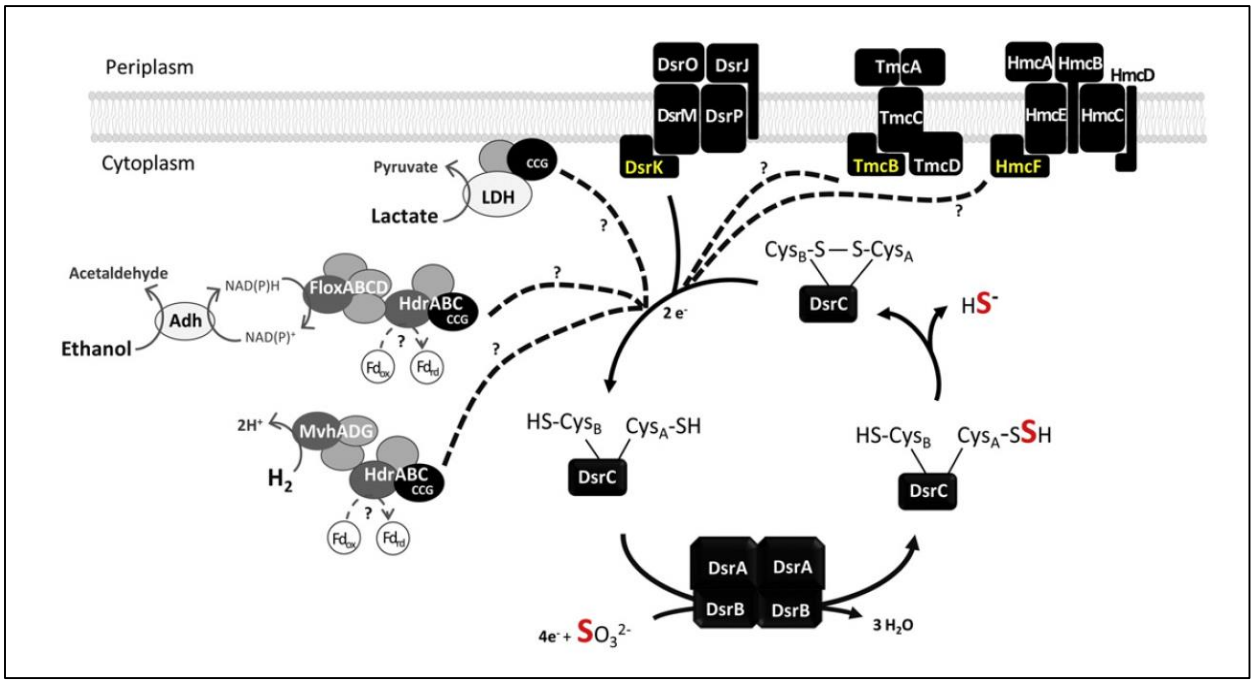

Figure 1.10 – Proposed model and possible physiological partners of DsrC in sulfite reduction of SRB. During sulfite reduction, after DsrC releases sulfide there's the formation of a disulfide between Cys_A and Cys_B. This disulfide bond is believed to be reduced by several proteins including the transmembrane complexes DsrMKJOP, HmcABCDEF and TmcABCD, and the soluble complexes FloxABCD/HdrABC, MvhDGA/ HdrABC and also Ldhs. Taken from (51).

Other set of conserved proteins related to HdrB/HdrD are lactate dehydrogenases which are encoded by three different gene loci. The first gene loci is involved in oxidation of organic acids and encodes, among other proteins, the Ldh catalytic subunit (*ldhA*), a Ldh iron-sulfur subunit with two CCG domains (*ldh1a*) and a HdrD related protein (*ldh1b*). The second gene locus has the genes *lldEFG* that encode a small HdrB related protein called LldE that contains two CCG domains. The third gene locus is constituted by two genes that encode the Ldh catalytic subunit (*ldhA*) and an HdrD-related protein encoded by the gene *ldh3*. These three gene loci encode Ldhs with HdrB/HdrD like subunits suggesting that they might transfer electrons to DsrC, coupling the oxidation of lactate to the reduction of sulfite (51).

Other Hdr-like proteins have also been identified such as the HdrD-related protein HdrF, which is a multidomain protein composed by an iron-sulfur domain, a transmembrane domain and two CCG domains, and HdrG which is a flavin adenine dinucleotide (FAD)-containing oxidoreductase containing a FAD-binding domain, one or two FAD oxidase domains, an iron sulfur domain and two CCG domains. Since these proteins have never been isolated their exact function is not yet known but it is suggested they are involved in electron transfer from NAD(P)H, fatty acids and other metabolites to oxidized DsrC or the MQ pool (51).

The possible interaction between DsrC and the membrane complexes DsrMKJOP, HmcABCDEF and TmcABCD might provide a connection between sulfite reduction and chemiosmotic energy conservation associated with proton translocations across the membrane, whereas the interaction of DsrC with the HdrABC soluble complexes may be associated with the energy coupling mechanism of electron bifurcation performed either by FloxABCD/HdrABC or MvhDGA/HdrABC (51).

Chapter II

Objectives

2. Objectives

It has been recently shown that DsrC is a central and important protein in the bioenergetic metabolism of sulfate reducers, namely by having a strong impact on sulfite reduction by DsrAB. Thus, the main objective of this project was to further study the role of this small protein in the sulfite reduction pathway and discover other possible interaction partners of DsrC.

This work focused on two objectives:

The first one was to investigate how DsrC impacts growth under sulfate reducing and fermentative conditions using *Desulfovibrio vulgaris* wild-type *versus* DsrC variant strains, using ethanol or pyruvate as electron donors. To achieve this objective growth studies of those strains were performed, aiming to elucidate the role of DsrC on the bioenergetic metabolism.

The second objective was to search for additional DsrC physiological partners during sulfate reduction while providing different electron donors such as lactate and ethanol. To achieve this objective DsrC pull down assays were performed in order to isolate DsrC in complex with other proteins. The co-eluted proteins were analysed by mass spectrometry, Sodium dodecyl sulfate-polyacrylamide gel electrophoresis (SDS-PAGE) and Western blot techniques.

Chapter III

Materials and Methods

3. Material and Methods

3.1. Growth Studies of DsrC Variant Strains

3.1.1. Strains

The strains used in this work were previously constructed in the lab (60) and are represented in Figure 3.1. The wild-type DVH (WT DvH) contains only the chromosomal copy of the *dsrC* gene (cDsrC). IPFG06 strain contains both the chromosomal and a plasmid copy of *dsrC* (pDsrC). IPFG07 strain contains only the plasmid-copy of *dsrC* and IPFG09 strain contains only the plasmid copy of *dsrC*, containing the Cys93Ala mutation in a strictly conserved cysteine, and a Cys26Ala mutation in a structural cysteine (not conserved among DsrC).

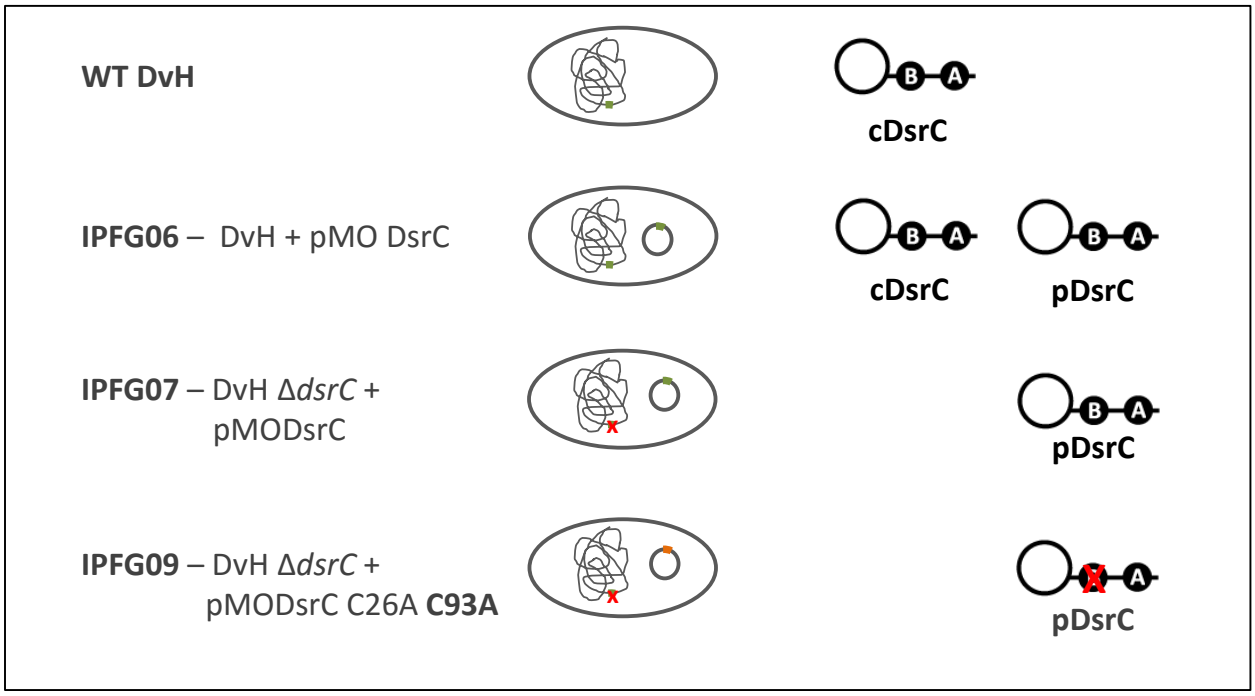

Figure 3.1 – Schematic representation of the different DvH strains used in this work.

3.1.2. Media

MOY medium used to grow all DvH strains contained 8 mM $MgCl_2$, 20 mM NH_4Cl, 0.6 mM $CaCl_2$, 2 mM K_2HPO_4-NaH_2PO_4, 0.6 % (v/v) Trace Elements, 0.06 mM FeCl, 0.12 mM EDTA, 30 mM Tris-HCl pH 7.4, 0.1 % (v/v) Thauers vitamins, 1 g/L yeast extract, 1.2 mM thioglycolate (used as a reducing agent), as described by Zane and coworkers (42). Trace Elements solution contained 2.5 mM $MnCl_2.4H_2O$, 1.26 mM $CoCl_2.6H_2O$, 1.47 mM $ZnCl_2$, 0.21 mM $Na_2MoO_4.2H_2O$, 0.024 mM $Na_2WO_4.2H_2O$, 0.32 mM H_3BO_3, 0.035 mM $Na_2SeO_3.5H_2O$, 0.012 mM $CuCl_2.2H_2O$ and 0.38 mM $NiCl_2.6H_2O$. Thauers vitamin solution contained 82 µM biotin, 45 µM folic acid, 468 µM pyridoxine hydrochloride, 148 µM thiamine hydrochloride, 133 µM riboflavin, 406 µM nicotinic acid, 210 µM DL-panthotenic acid, 365 µM *p*-aminobenzoic acid, 242 µM lipoic acid, 14 mM choline chloride, and 7.4 µM vitamin B12. The pH of the medium was adjusted with HCl to a final value of 7.2. All flasks and tubes were degassed with N_2, sealed and autoclaved to assure proper anaerobic growth. For different culture conditions MOY medium was supplied with different electron acceptors and donors. Pre-inoculum medium was provided with sodium pyruvate as an electron donor and sodium sulfate as an electron acceptor (60 mM pyruvate – 3 mM sulfate). MOY medium for ethanol-sulfate growth (respiration) was supplied with ethanol as an electron donor and sodium sulfate as an electron acceptor (40 mM ethanol – 20 mM sulfate). MOY medium for pyruvate growth (fermentation) was supplemented with sodium pyruvate as electron donor (60 mM pyruvate), and was provided with 3 mM sulfide working as a reducing agent and sulfur source. In this work ethanol-sulfate and pyruvate growth medium is going to be referred as MOY ES4 and MOY PYR, respectively.

3.1.3. Growth Curves

DvH WT and mutant strains were grown anaerobically at 37 ^oC. The experimental procedure to generate the growth curves is outlined in Figure 3.2. Hungate tubes containing MOY medium (60 mM Pyruvate – 3 mM sulfate) were inoculated with 1 mL of stock cells to a final volume of 5 mL (20 % (v/v) inoculum). Cells were grown overnight and then transferred into 100 mL flasks containing the same medium to a final volume of 50 mL (10 % (v/v) inoculum). The optical density (OD) of these pre-culture flasks was monitored until an OD_{600nm} of 0.6. Upon reaching the desired OD 100 mL flasks containing either MOY ES4 (40 mM ethanol – 20 mM sulfate) or MOY PYR (60 mM pyruvate) were inoculated with 4 % of these pre-cultured cells to a final volume of 50 mL. Antibiotics were added to MOY medium as follows: spectinomycin (100 µg/mL) was added to IPFG06, IPFG07 and IPFG09 strains in all growth steps and geneticin (400 µg/mL) was supplemented in pre-inoculum growths of IPFG07 and IPFG09. To the WT strain no antibiotics were added. The OD of the cultures was monitored at various time points with a Shimadzu UV-1603 spectrophotometer at 600 nm. All optical density measurements are the mean of three replicate experiments.

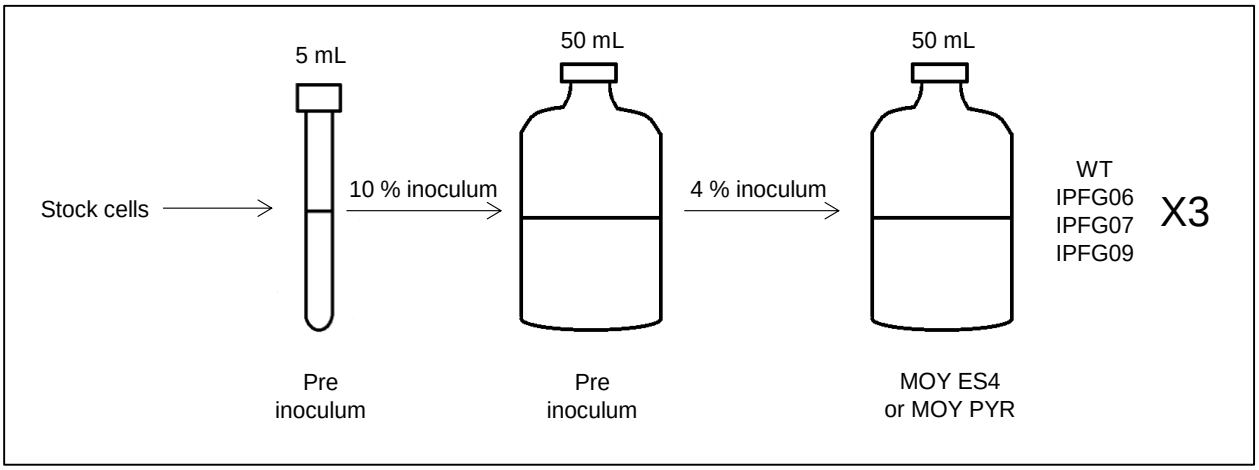

Figure 3.2 – Schematic representation of the experimental procedure used to monitor all growth curves.

3.1.4. Ethanol Quantification

Ethanol accumulation in the growth medium was determined with an enzymatic kit from NZYTech. This method is based on the quantification of NADH formed from ethanol through the combined action of alcohol dehydrogenase (Adh) and aldehyde dehydrogenase (AL-DH). First ethanol is oxidized by Adh with NAD^+ to form acetaldehyde and NADH (Eq. 1). AL-DH then oxidizes acetaldehyde with NAD^+ to produce acetate and NADH (Eq. 2). Since 2 molecules of NADH are created per molecule of ethanol, the quantification of NADH measured is twice the amount of ethanol in the sample.

$$\text{Ethanol} + NAD^+ \longrightarrow \text{Acetaldehyde} + NADH + H^+ \quad (1)$$

$$\text{Acetaldehyde} + NAD^+ + H_2O \longrightarrow \text{Acetate} + NADH + H^+ \quad (2)$$

The samples were collected from the flasks with MOY PYR growing strains at different time points (after inoculation, mid-exponential, late exponential, and stationary phase) and were centrifuged at 13000 rpm during 15 minutes to separate the cells from the medium. The enzymatic assay was performed in sealed cuvettes at room temperature and was processed in two steps. In the first step 50 µL of sample (or water for blank) was mixed with 1 mL of H_2O, 100 µL of potassium pyrophosphate buffer (1.5M, pH 9.0), 100 µL of NAD^+ and 10 µL of AL-DH (75 U/mL). Absorbance was then measured at 340 nm after 2 minutes (Abs1). In the second step 10 µL of Adh (167 U/mL) was added to the previous mixture and absorbance was again measured at the same wavelength after 5 minutes (Abs2).

Ethanol concentration was calculated by the absorbance difference for the blank and the samples (Abs2 – Abs1). The absorbance difference of the blank was subtracted from the absorbance difference of the sample thereby obtaining $\Delta Abs_{ethanol}$. The concentration of ethanol, based on the ε of NADH at 340 nm, was

calculated using the following expression: [Ethanol] (g/L) = 0.09287 × $\Delta Abs_{ethanol}$. All reported ethanol concentrations are the mean of three replicates.

3.2. Studies on DsrC Physiological Partners

3.2.1. Media and Cell Growth

To perform pull down assays using DsrC as a bait DvH WT and IPFG07 cells were grown either with ethanol or lactate as electron donors by using MOY ES4 medium (40 mM ethanol – 20 mM sulfate) or MOY LS4 medium (30 mM lactate – 30 mM sulfate), respectively. Cells were grown anaerobically at 37 ºC in 1 L reagent bottles using a final volume of 800 mL. All pre-culture cells were grown according to the procedure outlined in section 3.1.2. Reagent bottles were inoculated with 2 % (v/v) of fresh pre-cultured cells grown in MOY medium (60 mM pyruvate – 3 mM sulfate) as defined in Figure 3.3. Spectinomycin antibiotic was added to all tubes, flasks and reagent bottles growing IPFG07 cells. Pre-cultures of IPFG07 were also supplemented with geneticin. The OD of cultures was monitored at various time points with a Shimadzu UV-1603 spectrophotometer at 600 nm until they reached late exponential phase. Afterwards, cells were harvested by centrifugation at 13000 rpm for 15 minutes and the supernatant was discarded.

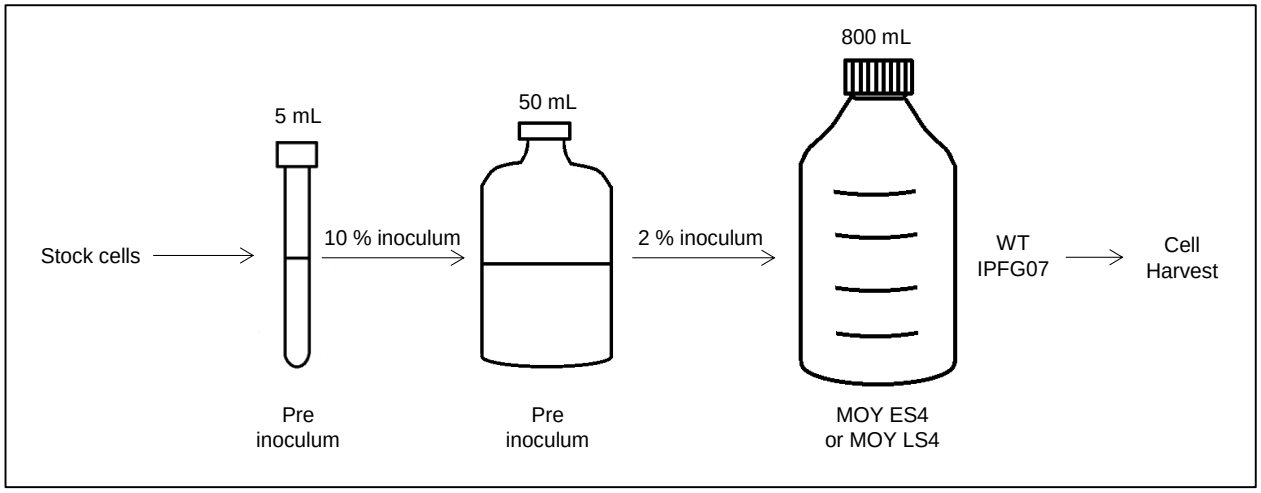

Figure 3.3 – Schematic representation of the experimental procedure used to grow WT and IPFG07 DvH cells for pull down assays.

3.2.2. DsrC Pull Down Assays

DsrC pull down assays were performed by affinity chromatography, specifically by immobilized metal ion affinity chromatography (IMAC), taking advantage of the His tag on plasmid-expressed DsrC from the IPFG07 strain. Harvested cells of DvH WT and IPFG07 grown either in MOY ES4 or MOY LS4 medium were resuspended in buffer A (25 mM potassium phosphate pH 7.4, 100 mM NaCl and 10 % glycerol) and disrupted in a French Press in the presence of DNase. The cell lysates were centrifuged for 20 minutes at 13000 rpm to remove cell debris (pellet) from the protein crude extract (supernatant) and this was then

ultra-centrifuged for 2 h at 42000 rpm to separate cell membranes (pellet) from the soluble fraction (supernatant). Before pull down assays, the total protein content of soluble fractions obtained from WT and IPFG07 cells was quantified using the Bradford method to ensure that the same amount of protein would be injected in the IMAC column (HiTrap Chelating HP column (GEHealthcare) charged with nickel). Using a FPLC AKTA^{TM} system the soluble fractions were injected into the column already equilibrated with buffer A. DsrC was then eluted with a mixture of buffer A and buffer B (25 mM potassium phosphate pH 7.4, 100 mM NaCl, 500 mM imidazole and 10 % glycerol) by using increasing concentrations of imidazole (30, 50, 70, 90, 110, 130, 150, 170, 200 and 500 mM). The chromatography was performed at 4 ºC. All fractions eluted were recovered and concentrated by centrifugation at 4000 rpm with concentrators using 3000 MW membranes (Millipore). Proteins eluted in each fraction were separated by SDS-PAGE (Sodium Dodecyl Sulfate-Polyacrylamide Gel Electrophoresis) and were then analyzed by mass spectrometry and Western blot.

3.2.3. Protein Quantification

Total protein concentration was determined by the Bradford method using a standard curve prepared with bovine serum albumin (NZYTech) in the following concentrations: 0, 125, 250, 500, 750 and 1000 µg/mL. The assay was prepared by mixing 20 µL of sample and 1 mL of Bradford reagent (Bio-rad). The blank was prepared by replacing sample with buffer A. Absorbance was then measured at 595 nm using a Shimadzu UV-1603 spectrophotometer.

3.2.4. Electrophoretic Techniques

Protein samples of each fraction obtained from the pull down assays were separated using Tricine-SDS-PAGE 10 % acrylamide (v/v). Each gel contained a stacking layer for protein concentration and a resolving layer for protein separation. To load the gels 20 µg of protein of each fraction was treated with the same volume of loading buffer (6 M Urea, 5 % w/v SDS, 0.1 % w/v glycerol, 0.05 % w/v bromophenol blue) and 1 µL of β-Mercaptoethanol and were then boiled for 4 minutes. The gels were run at 100 V for 30 minutes and after that 130 V for 2 hours using two different buffers: anode buffer (100 mM Tris pH 8.9) and cathode buffer (100 mM Tricine, 100 mM Tris and 0,1 % SDS pH 8.25). Lastly, the gels were stained using a Coomassie Blue solution.

The same protocol was used to separate proteins for Western blot analysis but instead of Tricine-SDS-PAGE 10 % acrylamide (v/v), Tricine-SDS-PAGE 13 % acrylamide (v/v) or SDS-PAGE 12 % acrylamide (v/v) was used depending on the proteins analyzed (see Table 3.1).

3.2.5. Mass Spectrometry Protein Identification

Mass spectrometry data was obtained by the Mass Spectrometry Unit (UniMS) at ITQB/iBET, Oeiras, Portugal. The protein bands were cut from the SDS-PAGE Coomassie Blue stained gels and then were de-stained, reduced with dithiothreitol, alkylated with iodoacetamide and digested with trypsin (Promega, 6.7 ng/µL) overnight at 37 ºC. The peptides were desalted and concentrated using POROS R2 (Applied Biosystems) and eluted directly onto the MALDI plate using 0.6 µL of 5mg/mL alpha-cyano-4-hydroxycinnamic acid (Sigma) in 50 % (v/v) acetonitrile and 5 % (v/v) formic acid. The data was acquired in positive reflector MS and MS/MS modes using a 4800plus MALDI-TOF/TOF (AB Sciex) mass spectrometer and the 4000 Series Explorer Software v.3.5.3 (Applied Biosystems). External calibration was performed using Pepmix1 (Laser BioLabs). The twenty-fifth most intense precursor ions from the MS spectra were selected for MS/MS analysis. The raw MS and MS/MS data was analyzed using Protein Pilot Software v. 4.5 (ABSciex) with the Mascot search engine (MOWSE algorithm). The searches were performed against the protein database NCBI (35149712 sequences; 12374887350 residues) with bacterial taxonomy restrictions (23117303 sequences). The search parameters were as follows: monoisotopic peptide mass values were considered, maximum precursor mass tolerance (MS) of 100 ppm and a maximum fragment mass tolerance (MS/MS) of 0.3 Da. A maximum of two tryptic missed cleavages were allowed. Carboxyamidomethylation of cysteines, oxidation of methionine, deamidation of asparagine and glutamine, and N-Pyro Glu of the N-terminal Q were set as variable modifications. Protein identification was only accepted when significant protein homology scores were obtained ($p<0.05$).

3.2.6. Western Blot Analysis

Protein samples were separated by SDS-PAGE [12 % acrylamide (v/v)] or Tricine-SDS-PAGE [13 % acrylamide (v/v)] and transferred to 0.45 µm polyvinylidene difluoride (PVDF) membranes (Roche) at 100 V and 400 mA in a Mini Trans-Blot® dry electrophoretic transfer cell (Bio-Rad) containing transfer buffer (48 mM Tris, 39 mM glycine pH 9.2). The type of SDS-PAGE gel and transfer time used for each protein is presented in Table 3.1. Protein volume to be loaded in the gel was calculated for each IPFG07 fraction and then the same volume was used for the corresponding WT fractions in order to calibrate the assay. The PVDF membranes were dried overnight, washed two times with TBS (Tris-Buffered Saline, 20 mM Tris-HCl pH 7.5, 150 mM NaCl) and then were treated with blocking buffer [20 mM Tris-HCl pH 7.5, 150 mM NaCl, 0.05 % Tween 20 (v/v), and 1 % nonfat milk (w/v)] and incubated with a primary antibody diluted in blocking buffer for 1 hour at room temperature. The dilutions of primary antibodies used were as follows: anti-FloxA at 1:3000, anti-HdrA at 1:1000, anti-Fdx at 1:1000, anti-Adh at 1:5000 and anti-Apr 1:3000 (see Table 3.1). After primary antibody incubation, membranes were washed three times and then incubated with anti-rabbit IgG antibody linked to alkaline phosphatase conjugate (Sigma-Aldrich®) at 1:15 000 dilution in blocking

buffer for 45 minutes at room temperature. After three washing steps with TBS, protein detection was performed using Alkaline Phosphatase Buffer (100 mM Tris-HCl pH 9.5, 100 mM NaCl, and 5 mM $MgCl_2$) and NBT (nitro-blue tetrazolium chloride)/BCIP (5-bromo-4-chloro-3-indolyl phosphate) substrates (Carl Roth®).

Table 3.1 – List of conditions used for Western blot analysis.

Primary/Secondary antibody	Gel used for protein separation	Total Protein mass loaded (µg)	Transference time (min)	Primary/Secondary antibody dilution
Anti-FloxA/Anti-rabbit IgG	SDS-PAGE 12 % acrylamide (v/v)	10	30	1:3000/1:15000
Anti-Adh/Anti-rabbit IgG	SDS-PAGE 12 % acrylamide (v/v)	10	30	1:5000/1:15000
Anti-HdrA/Anti-rabbit IgG	SDS-PAGE 12 % acrylamide (v/v)	10	30	1:1000/1:15000
Anti-Apr/Anti-rabbit IgG	SDS-PAGE 12 % acrylamide (v/v)	10	30	1:3000/1:15000
Anti-Fdx/Anti-rabbit IgG	Tricine-SDS-PAGE 13 % acrylamide (v/v)	40	7	1:1000/1:15000

Chapter IV

Results

4. Results

4.1. Growth Curves of DsrC variant Strains

In order to study the impact of DsrC in cell growth, three DsrC variant strains were used (as described in Figure 3.1) alongside with WT DvH strain: Strain IPFG06 which is the WT strain complemented with a plasmid containing the *dsrC* gene that encodes the DsrC protein with a 6 histidine tag tail at the N-terminus (WT + pMOIPHisDsrC), strain IPFG07 strain constructed by deleting the chromosomal *dsrC* gene from IPFG06 (DvH Δ*dsrC*::Km^R + pMOIPHisDsrC), and strain IPFG09 strain also lacking the chromosomal *dsrC* gene and containing a plasmid encoding DsrC with a mutation in Cys93 that was mutated for an alanine (DvH Δ*dsrC*::Km^R + pMOIPHisDsrCC26AC93A). All these strains were previously characterized for lactate/sulfate growth conditions, which are standard conditions for DvH, in order to evaluate the effect on sulfate reduction. Here, the same strains were grown in two other different media, MOY ES4 for anaerobic respiration with ethanol as an electron donor and sulfate as electron acceptor (Figure 4.1 A), and MOY PYR for fermentative growth in which pyruvate was given as an electron donor (Figure 4.1 B). These conditions are an extension of growth studies already run in the lab and will allow to better evaluate the physiological function of the DsrC protein.

In ES4 medium, the WT and IPFG06 strains had a similar growth behavior, showing very similar growth rates and cell duplication times as shown in Figure 4.1 A and Table 4.1. IPFG07 showed a growth rate about 20 % inferior to the WT strain, which means that in this condition the cell growth is slightly affected. This result can be explained by the fact that DsrC is expressed at a lower level in the IPFG07 strain when compared to WT and IPFG06, which leads to a slower cell growth (60). Among all the strains used, IPFG09 was the one most affected, showing a growth rate more than two times inferior than WT. When looking to the maximum OD reached, WT, IPFG06 and IPFG07 strains achieved similar values, while IPFG09 clearly grew less than the others. In PYR medium all strains reached lower ODs when compared to growth in ES4 medium (Figure 4.1.B), as no electron acceptor was provided to support anaerobic respiration and cells grew fermentatively. In this medium, surprisingly, the IPFG06 strain was not able to grow which suggests that for some unknown reason this strain was unstable in this condition, since the IPFG07 strain was able to grow. IPFG07 showed slightly increased cell duplication time when compared to the WT strain while IPFG09 strain displayed a much higher duplication time and much smaller growth rate and maximum OD. Furthermore, the IPFG09 strain was only able to double its OD about one time whereas WT could double its OD about six times, showing that IPFG09 strain was practically impaired. These growth differences between IPFG09 strain and the other strains indicates that DsrC, and in particular its Cys93, is not only important in sulfate respiration, where it has a critical role in dissimilatory sulfite reduction, but also in fermentative growth since a point mutation in one cysteine causes such a decrease in cell growth, evidenced by the comparison of the strains IPFG07 and IPFG09.

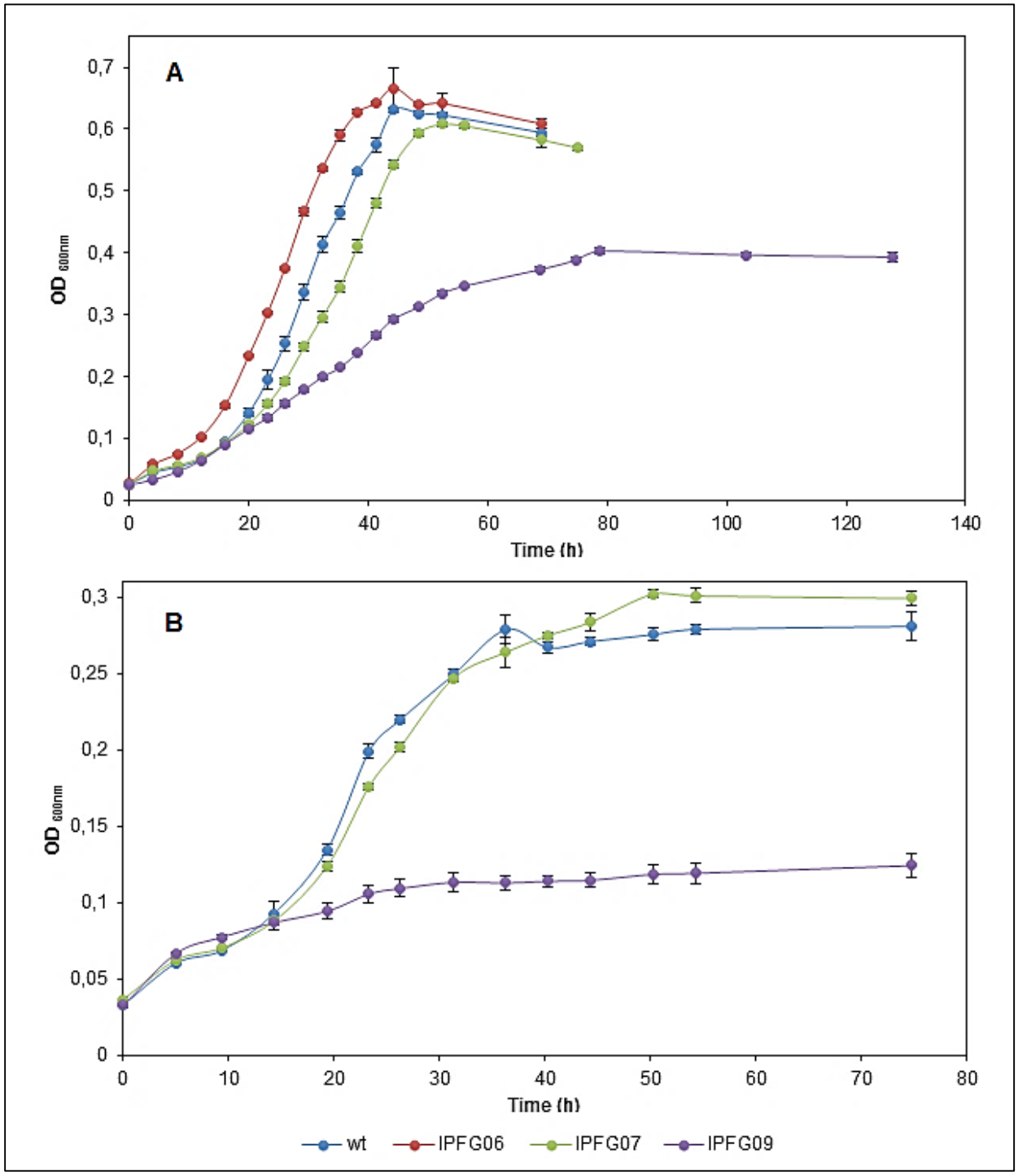

Figure 4.1 – Growth curves of DVH WT and DsrC variant strains in (**A**) ethanol-sulfate (40 mM/20 mM) and (**B**) pyruvate (60 mM) fermentation conditions. The points are the mean of three replicates, and error bars are relative to standard deviations. WT – DvH wild-type; IPFG06 – WT + pMOIPHisDsrC; IPFG07 – DvH Δ*dsrC*::Km^R + pMOIPH-isDsrC; IPFG09 – DvH Δ*dsrC*::Km^R + pMOIPHisDsrCC26AC93A.

Table 4.1 - Specific growth rate (μg), doubling time (Td), and maximum OD (600 nm) for DVH WT and DsrC variant strains in different conditions: ethanol-sulfate [ES4 (40 mM - 20 mM)] and pyruvate [PYR (60 mM)]; WT – DvH wild-type; IPFG06 – WT + pMOIPHisDsrC; IPFG07 – DvH Δ*dsrC*::Km^R + pMOIPHisDsrC; IPFG09 – DvH Δ*dsrC*::Km^R + pMOIPHisDsrCC26AC93A.

Medium	**ES4 (40 mM/20 mM)**			**PYR (60 mM)**		
Strain	μ_g (h^{-1})	T_d (h)	Max. OD_{600}	μ_g (h^{-1})	T_d (h)	Max. OD_{600}
WT	0.09±0.002	7.8±0.2	0.632±0.001	0.07±0.002	9.6±0.3	0.281±0.008
IPFG06	0.09±0.002	8.0±0.2	0.667±0.030	---	---	---
IPFG07	0.07±0.001	10.3±0.2	0.608±0.004	0.06±0.001	11.4±0.2	0.302±0.003
IPFG09	0.04±0.003	15.3±1.1	0.403±0.005	0.02±0.001	29.5±4.4	0.124±0.004

Ethanol has shown to be a metabolic product of DvH, produced in higher amounts with pyruvate as an electron donor. In a previous study conducted by Ramos *et al.,* the DvH WT strain grown during pyruvate fermentation was able to accumulate ethanol but not the mutants lacking the *hdrC* or *floxA* genes (58). To check whether DsrC is also involved in the production of ethanol as a fermentative product during growth on pyruvate, ethanol accumulated in the growth media of the WT and DsrC variant strains was quantified (Figure 4.2). Samples were recovered after inoculation (0 h), mid exponential (23 h), late exponential (50 h) and at stationary phase (74 h). Surprisingly, the IPFG09 strain which demonstrated the lower cell growth was the one to accumulate the higher amounts of ethanol, and even IPFG07 strain which express less quantity of DsrC than the WT strain produced more ethanol overtime. This means that the mutation created in the Cys93 of DsrC and low expression of DsrC somehow contributes to a higher production of ethanol.

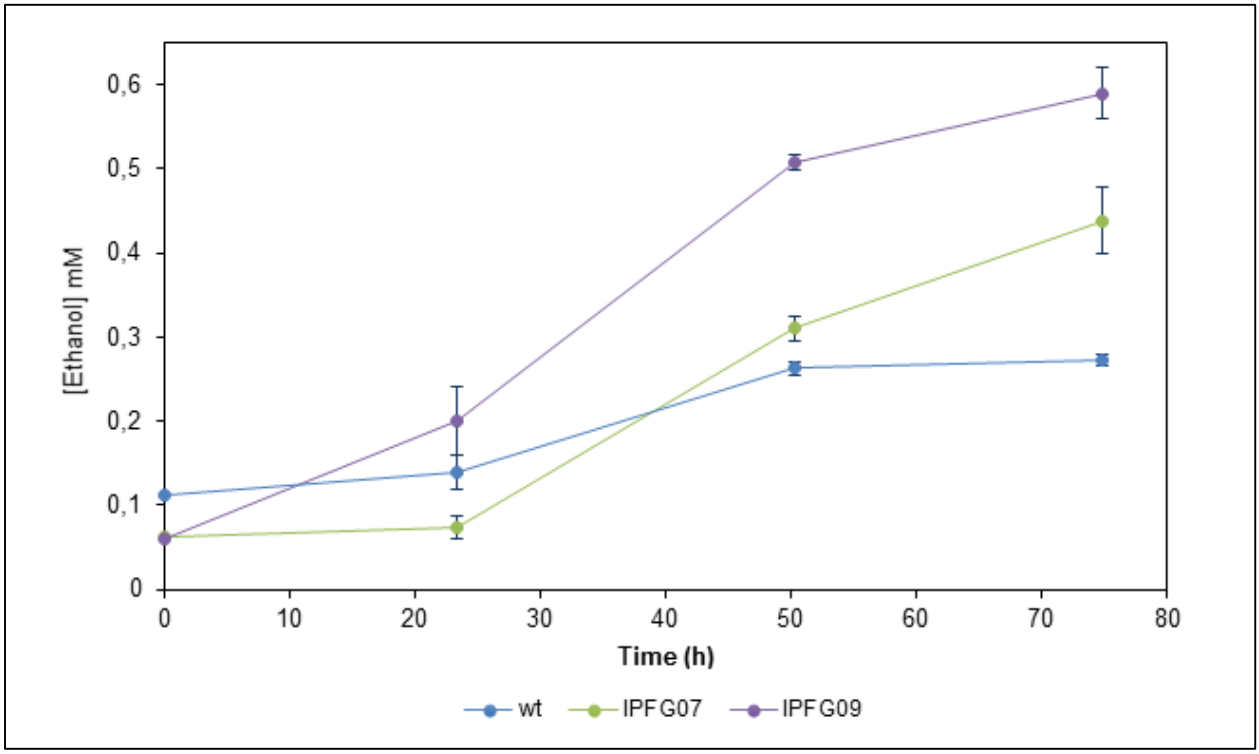

Figure 4.2 – **Ethanol (mM) accumulated during growth of DvH WT and DsrC variant strains during pyruvate fermentation** [PYR (60 mM)]*;* WT – DvH wild-type; IPFG06 – WT + pMOIPHisDsrC; IPFG07 – DvH Δ*dsrC*::Km^R + pMOIPHisDsrC; IPFG09 - DvH Δ*dsrC*::Km^R + pMOIPHisDsrCC26AC93A. The points are the mean of three replicates and error bars are relative to standard deviation.

4.2. DsrC physiological partners

In order to identify the possible physiological partners of DsrC in sulfite reduction pull down assays with DsrC were performed using affinity chromatography. For these experiments, the aim was to find HdrB and HdrD-like proteins that possibly give electrons to DsrC during the bioenergetic metabolism. The pull down assays were performed using the soluble fraction of the WT and IPFG07 strains grown either in ES4 or LS4 medium. The IPFG07 strain expresses DsrC with a histidine tag at the N-terminus, which enables its binding to the affinity resin. The WT strain served as a control, to identify the proteins that interact non-specifically with the matrix of the resin. The LS4 medium was used with the goal to find several lactate dehydrogenases (Ldh1a, Ldh1b, LldEFG and Ldh3) that are possibly involved in electron transfer to DsrC during lactate oxidation or even HdrG (DVU3071 and DVU0253), which is reported to be upregulated in lactate-thiosulfate conditions (see Table 4.2) (51). Then, the purpose of using the ES4 medium was to possibly identify the HdrABC/FloxABC complex (see Table 4.2) which was previously suggested to work together with Adh and DsrC in ethanol oxidation, and studies of gene and protein expression of FloxA and HdrA revealed that these are more expressed under ES4 condition, making this condition more prone to find these candidates (58).

Table 4.2 – **Possible soluble physiological partners of DsrC in DvH according to literature.** The proteins presented here are related to HdrB and HdrD present in methanogens.

	HdrB-like proteins	**HdrD-like proteins**					
	HdrB from HdrABC/FloABCD	Ldh1a	Ldh1b	LldE	Ldh3	HdrG	
Locus Tag	DVU2403	DVU3028	DVU3033	DVU1783	DVU0826	DVU3071	DVU0253
Mass (kDa)	35	46	80	28	48	131	103

The pull down assays were performed using an IMAC column loaded with nickel, since histidine has a high affinity for this metal. The DsrC expressed by IPFG07 strain, together with its physiological partners, were bound to the column taking advantage of the histidine tail present at the N-terminus of DsrC. After that, DsrC and its partners were eluted using successively increasing concentrations of imidazole. This solvent competes with the histidine tag tail of DsrC for binding to the column and replaces it, eluting DsrC and possibly its interaction partners that were aimed to be identified in this work.

The fractions obtained for each imidazole concentration used to elute DsrC were analyzed using SDS-PAGE as presented in Figure 4.3. It can be observed that for fractions acquired from the WT pull down assays (Figure 4.3 A and 4.3 C for ES4 and LS4 conditions, respectively), the bands correspond to proteins that have some affinity for nickel and that were slowly eluted from the column with imidazole, since DsrC does not bind to the affinity column. Regarding the fractions obtained from the pull down assays of the IPFG07 strain (Figure 4.3 B and 4.3 D for ES4 and LS4 conditions, respectively) it can be observed that DsrC elutes from the column mainly between 90 to 110 mM of imidazole. This can be observed by the DsrC band that appears close to 14 kDa, which has a higher intensity in those fractions. The already-known physiological partner of DsrC, the sulfite reductase DsrAB, was easily identified by the two intense bands that appear near 50 kDa and 40 kDa for DsrA and DsrB subunits, respectively (as indicated in Figure 4.3 B and Figure 4.3 D). It can also be noted that the fractions with the higher amounts of DsrC are different for LS4 and ES4 conditions, which suggests that the proteins expressed and that are pulled down with DsrC in these two conditions are not the same.

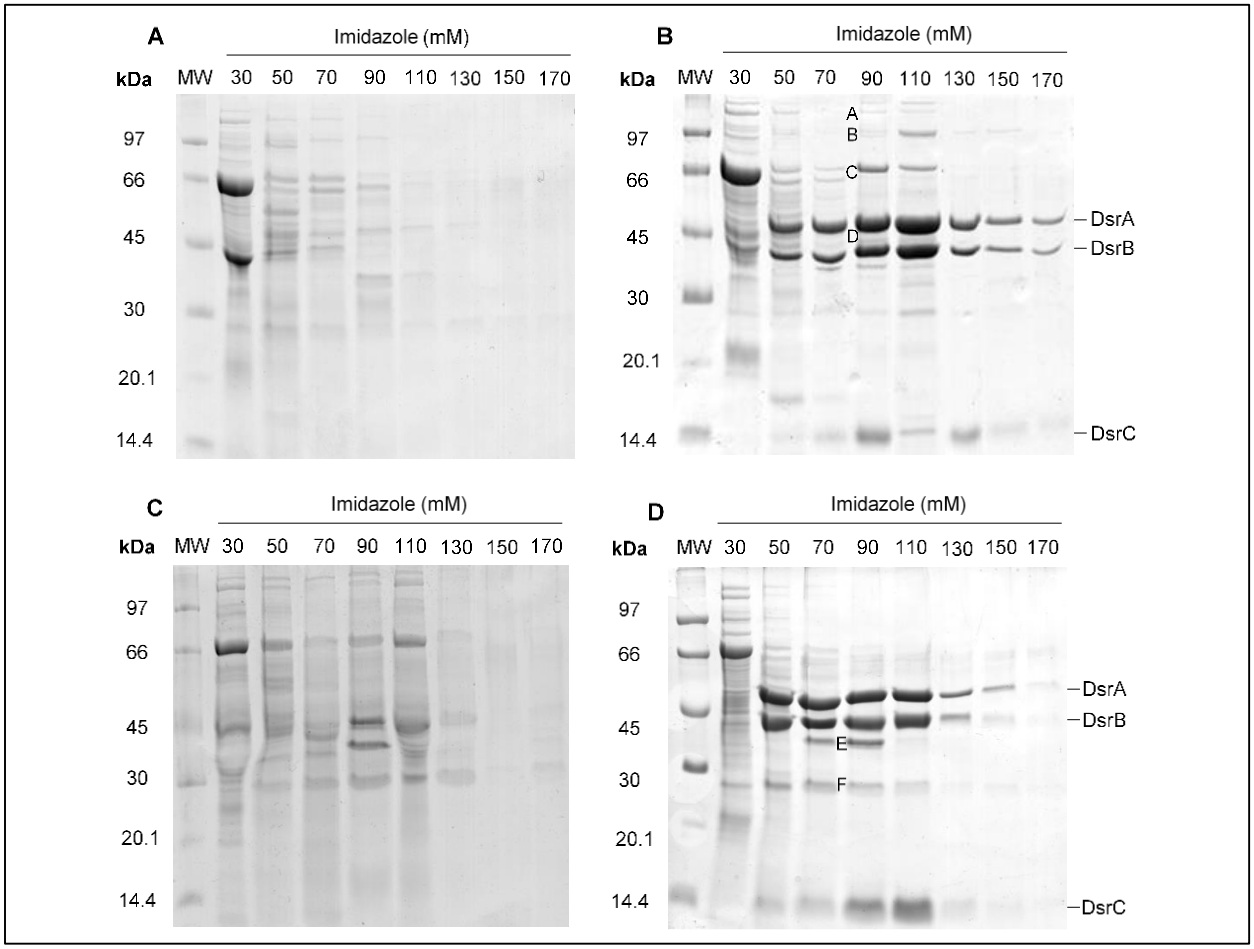

Figure 4.3 – **Tricine-SDS-PAGE 10 % acrylamide protein separation of the fractions obtained from the DsrC pull down assays** using WT soluble fractions of cells grown in ES4 (**A**) or LS4 medium (**C**) and IPFG07 soluble fractions of cells grown in ES4 (**B**) or LS4 medium (**D**). Each lane was loaded with 20 µg of protein of different fractions obtained through the pull downs using 30, 50, 70, 90, 110, 130, 150 and 170 mM of imidazole.

4.2.1. Mass Spectrometry

In order to identify the possible protein partners of DsrC, the main bands from the fractions eluted at 90 mM of imidazole were identified by mass spectrometry having in mind the molecular weights of the possible partners of DsrC presented in Table 4.2 (see Table 4.3). From the LS4 growth condition (Figure 4.3 D) no proteins related to sulfite reduction or belonging to the HdrB or HdrD-like protein group were identified. In the case of the ES4 growth condition (Figure 4.3 B) it was possible to identify APS reductase (AprA), which is involved in the reduction of APS to sulfite in dissimilatory sulfate reduction, and an iron-sulfur alcohol dehydrogenase (together with DsrB and AprA in the same band) responsible for the oxidation of ethanol to acetaldehyde. This alcohol dehydrogenase may be involved in the electron bifurcation mechanism conducted by the soluble complex FloxABCD/HdrABC to reduce Fdx and possibly DsrC, as it was proposed by Ramos *et al*. (58).

Table 4.3 – **Mass spectrometry analysis of the proteins bands cut from the SDS-PAGE gels.** Bands are identified in Figure 4.3. Only proteins with the best score are presented here except band D where Adh1, with the best score, was identified with two other proteins (DsrB and AprA) with a lower score.

Band	Protein	Locus Tag	Mass (kDa)
A	Phosphoenolpyruvate synthase	DVU1833	132
B	Sensory box histidine kinase/response regulator	DVU3045	104
C	Adenylylsulfate reductase subunit alpha (AprA)	DVU0847	74
D	Iron-containing alcohol dehydrogenase (Adh1) Dissimilatory sulfite reductase subunit beta (DsrB) Adenylylsulfate reductase subunit alpha (AprA)	DVU2405 DVU0403 DVU0847	42 42 74
E	Cation ABC transporter periplasmic-binding protein	DVU1343	36
F	Nickel transport complex	DVU0949	27

4.2.2. Western Blot Analysis

The protein fractions obtained from DsrC pull downs assays using IPFG07 and WT (control) cell extracts were analyzed by Western blot. As Adh1 was found by mass spectrometry in a protein fraction where DsrC was eluted, this result prompted the search for the FloxABCD/HdrABC complex with whom Adh1, DsrC and Fdx are proposed to work with, as described by Ramos *et al.* (58). The Western blot assays were performed with antibodies against the following proteins: Adh, Apr, FloxA, HdrA, and Fdx. First, Western blot against Aps reductase (AprBA) and alcohol dehydrogenase (Adh) were analyzed to confirm the results obtained from mass spectrometry. The Western blot against Apr (Figure 4.4 A) showed that in the fraction where DsrC is eluted from the column (90 mM of imidazole) the band intensity for Apr is higher than in the equivalent fraction of the control. This result validates the previous data from mass spectrometry. In the case of the Western blot against Adh (Figure 4.4 B) the results were similar to the ones obtained for Apr. In WT fractions, the Adh response decreases with the increase of imidazole concentration, showing that it binds non-specifically to the column, whereas in the IPFG07 strain the protein level increases with the increase of imidazole concentration. In the IPFG07 strain the fraction where DsrC is eluted (90 mM of imidazole) is where the band intensity for Adh is higher and also higher than in the WT counterpart.

Since it was possible to successfully identify Adh together with DsrC in ES4 condition using mass spectrometry and Western blot, it was then decided to perform additional Western blot analysis against proteins that may be part of the soluble FloxABCD/HdrABC complex. To identify the FloxABCD protein the antibody against FloxA was used and to detect the HdrABC protein the antibody against HdrA was used. Additionally, Western blot against Fdx was performed, since the FloxABCD/HdrABC complex is proposed to reduce both ferredoxin and DsrC. When comparing protein fractions from the pull down assays performed with the WT and IPFG07 cell extracts eluted at 90 mM of imidazole using the antibody against FloxA, the result is very

evident, there is a much stronger response in the IPFG07 strain than the WT, which is almost absent (Figure 4.4 C and Figure 4.5 C). This very clear result suggests that FloxABCD works as a physiological partner or part of the complex that interacts with DsrC. In HdrA Western blot (Figure 4.4 D) the difference in band intensity between IPFG07 and WT fractions eluted at 90 mM of imidazole is not so evident, but measurement of relative band intensities (Figure 4.5 D) revealed that the response is higher in the IPFG07 strain. Finally, in the Fdx Western blot, comparison of the fractions eluted at 90 mM of imidazole also revealed a higher response for IPFG07 when compared to the WT. All together these results show that Adh, Flox, Hdr and Fdx co-elute with DsrC and thus are likely to form a physiological complex with it that might channel electrons from the oxidation of ethanol to DsrC, as suggested previously by Ramos *et al.* (58). The same proteins were also analyzed for the LS4 growth condition. However, the results obtained were not so evident which comes in agreement with FloxABCD/HdrABC complex being essential proteins for ES4 conditions but not for LS4 conditions (58).

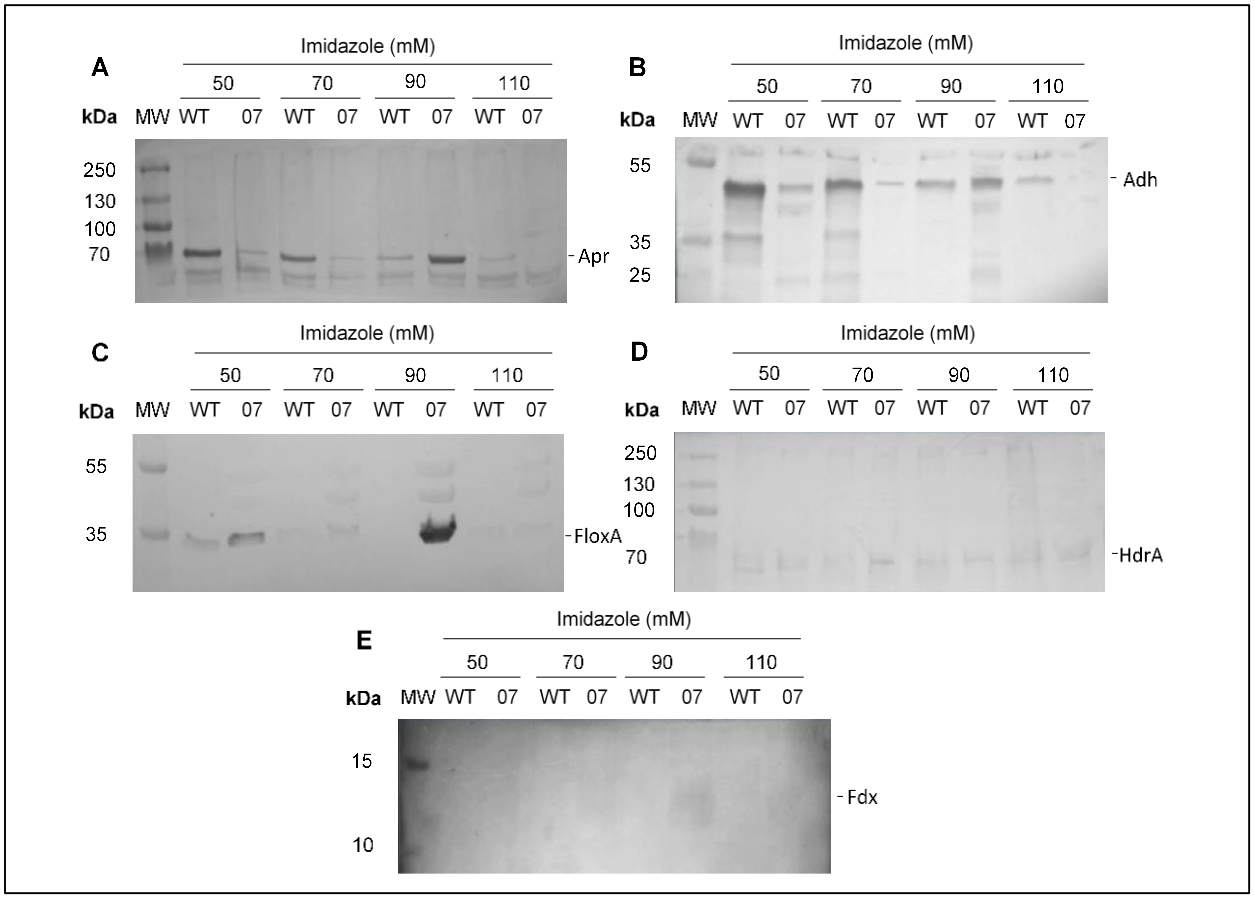

Figure 4.4 – **Western Blot analysis of protein fractions obtained from DsrC pull down assays of the soluble fraction of cells grown in ES4 medium.** WT and IPFG07 fractions eluted with 50, 70, 90 and 110 mM of imidazole were loaded into a SDS-PAGE gel and transferred to a PVDF membrane. Antibodies and dilutions used were as follows: anti-Apr at 1:3000 (**A**), anti-Adh at 1:5000 (**B**), Anti-FloxA at 1:3000 (**C**), anti-HdrA at 1:1000 (**D**) and anti-Fdx at 1:1000 (**E**).

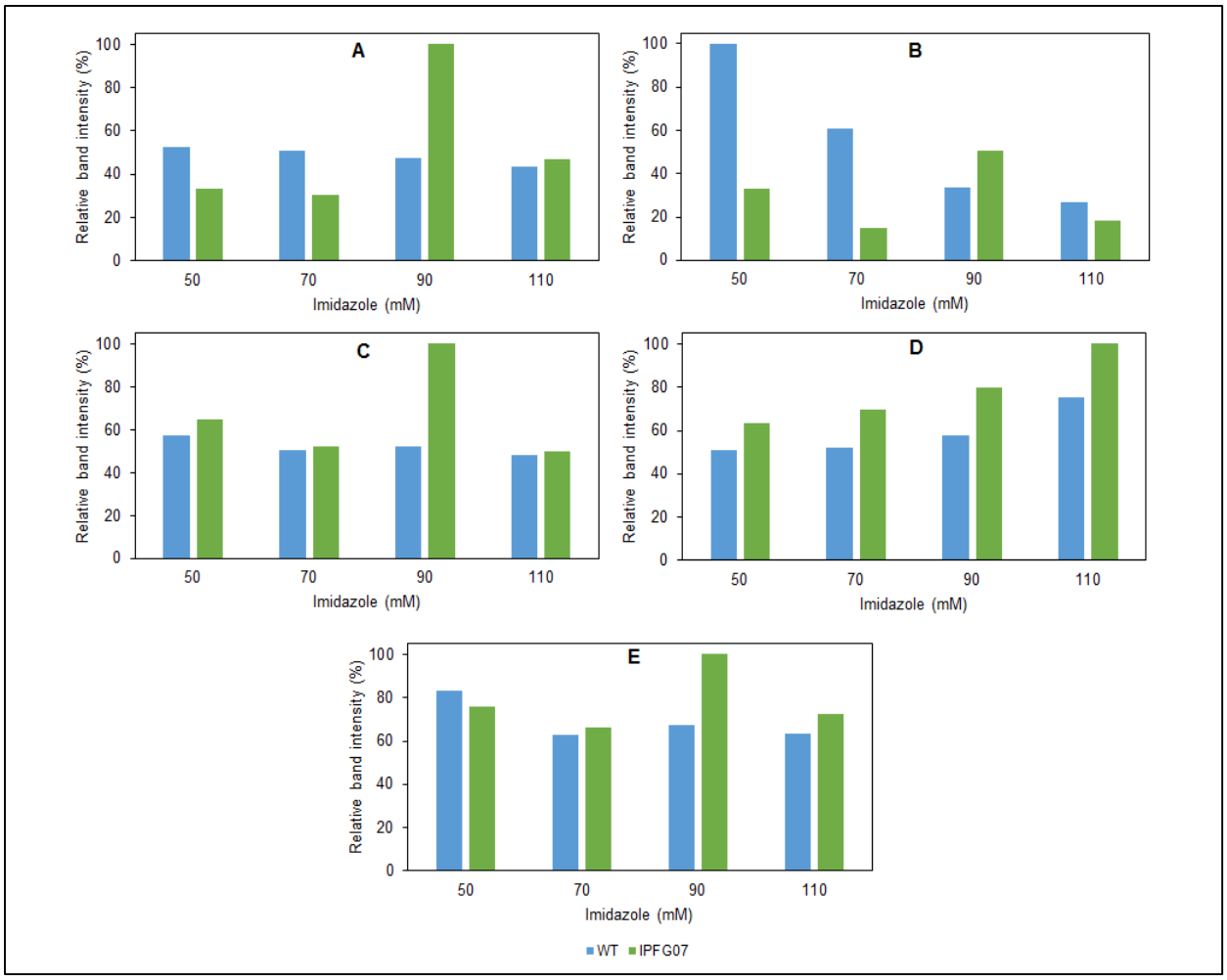

Figure 4.5 – Relative band intensity of the proteins bands analyzed by Western blot. Band intensity measurements of the proteins analyzed by Western blot were performed for each fraction from WT and IPFG07 strains eluted with 50, 70, 90 and 110 mM imidazole. **(A)** Apr, **(B)** Adh, **(C)** FloxA, **(D)** HdrA and **(E)** Fdx.

Chapter V

Discussion

5. Discussion

A microbial basis for IBD has long been suspected, and potential infectious agents associated with UC and CD have been the target of study for many years (61). The implication of SRB in IBD has been suggested since their metabolic end product, hydrogen sulfide, is a cytotoxic compound and may trigger an excessive immune response in genetic susceptible hosts that can lead to chronic inflammation of the intestinal tissue and epithelium cell death (15). The study of the metabolism of these microorganisms becomes of extreme relevance since the changes they cause within the gut are very important in sustaining these diseases, promoting the development of long term complications and being also responsible for poor responses to certain therapeutic approaches (61).

The aim of this work was to further study the impact of the protein DsrC during dissimilatory sulfate reduction and pyruvate fermentation, trying also to identify its possible physiological partners during sulfite reduction to sulfide. In dissimilatory sulfate reduction, DsrAB is the protein responsible for reducing sulfite to sulfide. This step also requires the presence of DsrC, and its two highly conserved C-terminal cysteines have been shown to be involved in the sulfite reduction mechanism. This protein is also suggested to have an important role in cellular metabolism by the fact that it is a very highly expressed protein in the model DvH being expressed at similar or even higher levels than other proteins involved in sulfate reduction (51).

In this work, growth studies performed with DvH DsrC variant strains also showed that DsrC is of major importance in the energy metabolism of these microorganisms. When using ES4 growth condition, the WT and IPFG06 strains grew very similarly, but IPFG07 and IPFG09 strains displayed higher duplication times and reached lower OD values. The lower expression levels of the plasmid-encoded DsrC in the IPFG07 strain relative to the levels expressed by the WT chromosomal *dsrC* gene can explain the slightly increased cell doubling time i.e. decreased cell growth rate and maximum OD observed for this strain. In IPFG09 strain, the decrease in growth rate and much lower OD obtained are the result of a single point mutation in one of the highly conserved cysteines (Cys93) present in the flexible C-terminal arm of DsrC indicating a crucial role of this cysteine in sulfite reduction. During pyruvate fermentation, the lower expression of DsrC also affected growth of IPFG07, but the mutation introduced in Cys93 of DsrC (IPFG09 strain) had an even more pronounced effect in this condition when compared to ES4, since the OD was only able to double once. This suggests that DsrC may have another role during pyruvate fermentation besides sulfite reduction as cells are not using sulfate for respiration during pyruvate fermentation.

These findings support the fact that DsrC has a major impact in the bioenergetics of SRB, as previously reported when growing the same strains on lactate instead of ethanol as an electron donor (60). In LS4 condition it was observed that the WT and IPFG06 strains reach very similar ODs, but IPFG07 and IPFG09 strains have their growth clearly affected, with IPFG09 being the most affected one due to the Cys93 point mutation (Table 5.1) (60). The results obtained in this work for ES4 condition are thus in agreement with

the data previously obtained. When comparing cell doubling times it is observed that in LS4 condition the IPFG09 strain has a doubling time about 1.2 times higher than IPFG07 strain, whereas in ES4, when comparing the same strains, the cell duplication time is about 1.5 times higher. Besides doubling time, the maximum OD reached in the IPFG09 strain showed that this strain is more affected in ES4 than in LS4 comparatively to IPFG07 strain, suggesting that Cys93 of DsrC may not be only involved in the reduction of sulfite but also in the ethanol-oxidation metabolism.

Table 5.1 - Doubling time (Td) and maximum OD (600 nm) for *D. vulgaris* WT and DsrC variant strains in LS4 (60 mM lactate – 30 mM sulfate) condition. wt **–** DvH wild-type; IPFG06 **–** WT + pMOIPHisDsrC; IPFG07 **–** DvH Δ*dsrC*::Km^R + pMOIPHisDsrC; IPFG09 - DvH Δ*dsrC*::Km^R + pMOIPHisDsrCC26AC93A. Taken from (60).

Strain	T_d (h)	Max. OD_{600}
WT	2.7±0.1	0.955±0.006
IPFG06	3.6±0.1	0.952±0.003
IPFG07	7.0±0.1	0.807±0.005
IPFG09	8.6±0.2	0.667±0.008

To further study the role of DsrC in pyruvate fermentation conditions, ethanol accumulation was measured over time. Ethanol has been reported as a metabolic product of DvH when pyruvate is used as an electron donor for fermentation. In a previous work the DvH WT strain accumulated ethanol, while strains lacking the *floxA* and *hdrC* genes did not (58). Thus, the same experiment was performed with DsrC variant strains, but the results were not similar. First, in this work the ethanol accumulated over time in the WT strain was much lower than the ethanol accumulated in the WT strain of that work (58). This result can be explained by the fact that the growth conditions are not exactly the same, as in this work the strains were grown in a true fermentative state (there was no addition of sulfate to support respiration), whereas in the previous study the growth media was supplemented with 3 mM of sulfate. These might explain the differences in ethanol accumulation measured. Moreover, in that work ethanol accumulation only started when the strains reached stationary phase while here ethanol accumulation accompanied throughout cell growth. In this work, the WT strain only accumulated a small amount of ethanol, whereas IPFG07 strain, which has a lower expression of DsrC and IPFG09 strain with a point mutation in DsrC were accumulated higher amounts of ethanol than the WT. This suggests that DsrC is not involved in ethanol production by FloxABCD/HdrABC complex as it was proposed by Ramos *et al.* (Figure 5.1 B) (58), but DsrC might influence the ethanol production throughout another indirect pathway not yet identified. We can speculate that the DsrC influence can be at the level of gene regulation since this protein contains a HTH motif (Figure 1.7) (51) or due to DsrC Cys that can change the intracellular redox potential to more negative potential that will favor Fdx to

be in a more reduced form and, consequently, favor the ethanol production through Flox/Hdr complex. Thus, the role of DsrC under pyruvate fermentation condition requires further experimental work.

The dissimilatory reduction of sulfate in SRB is not fully elucidated yet, and questions like who provides electrons for the reduction of DsrC during sulfite reduction remain to be answered. In order to clarify this question it was searched for physiological partners of DsrC using pull down assays coupled with identification by mass spectrometry and Western blot analysis. The data show that FloxA, HdrA, Adh and Fdx co-elute together with DsrC in ES4 conditions suggesting that the complex FloxABCD/HdrABC together with Adh and Fdx work together and with DsrC, as previously suggested by Ramos *et al.* (58). In addition, APS reductase was also found to co-elute with DsrC, a result confirmed both by mass spectrometry and Western blot. This was already observed in a previous study where pull downs assays were performed using AprA as a bait and DsrC was found to co-elute with it (62). There is no evidence that support the idea that DsrC is involved in the reduction of APS to sulfite. On the other side, DsrC, together with DsrAB, could form a supramolecular structure with Apr, as it happens with other proteins like lactate-dehydrogenase and pyruvate-ferredoxin oxidoreductase during lactate oxidation (63). This supramolecular structure would bring together enzymes involved in sulfate reduction facilitating substrate channeling between them. However additional studies should be performed to support this suggestion.

In *D. vulgaris*, the *flox-hdr* gene cluster is present upstream of an alcohol dehydrogenase coding gene (*adh1*), which is highly expressed in *D. vulgaris* grown with lactate, pyruvate, formate, ethanol or hydrogen as electron donors for sulfate reduction (57). Previously, a *D. vulgaris* mutant lacking the *adh* gene was unable to grow in ethanol-sulfate medium (57) and the same was found regarding DvH strains lacking the *floxA* and *hdrC* genes (58). This means that these proteins are crucial enzymes in ethanol oxidation. The probable pathway involving Adh1 and Flox-Hdr proteins starts with the oxidation of ethanol to acetaldehyde by Adh1. The electrons released by ethanol oxidation are used to reduce NAD^+ to NADH, which then binds to the NAD(P) binding domain of FloxA. This protein then oxidizes NADH and the electrons are transferred from FloxA to FloxB and FloxCD. After this, the electrons are conducted to HdrABC and then used to reduce DsrC and Fdx, as proposed by Ramos and coworkers (Figure 5.1 A) (58). The experimental results obtained here provide evidences, for the first time, that DsrC indeed interacts with the Flox-Hdr complex and may be its physiological partner. Additionally, the interaction between DsrC, Adh and the FloxABCD/HdrABC complex provides a connection between the sulfate reduction pathway and carbon metabolism for energy conservation in SRB (Figure 5.2). The energy coupling mechanism of FloxABCD/HdrABC was proposed to be based on electron bifurcation, where the endergonic reduction of Fdx is coupled to the exergonic reduction of DsrC. This suggestion gains further support by the decreased growth of the DsrC mutant strains during ethanol oxidation observed in this work.

The interaction between FloxABCD/HdrABC and DsrC was also analyzed using lactate-sulfate grown cells but it was not possible to be detect it using lactate as an electron donor to sulfate reduction. This can be explained by a previous study performed by Ramos *et al.* (58) where the expression levels of *floxA* and *hdrA* genes were shown to be higher when using ethanol as electron donor over lactate. Thus, the low expression level of FloxA and HdrA probably explain why they could not be found together with DsrC in the LS4 condition.

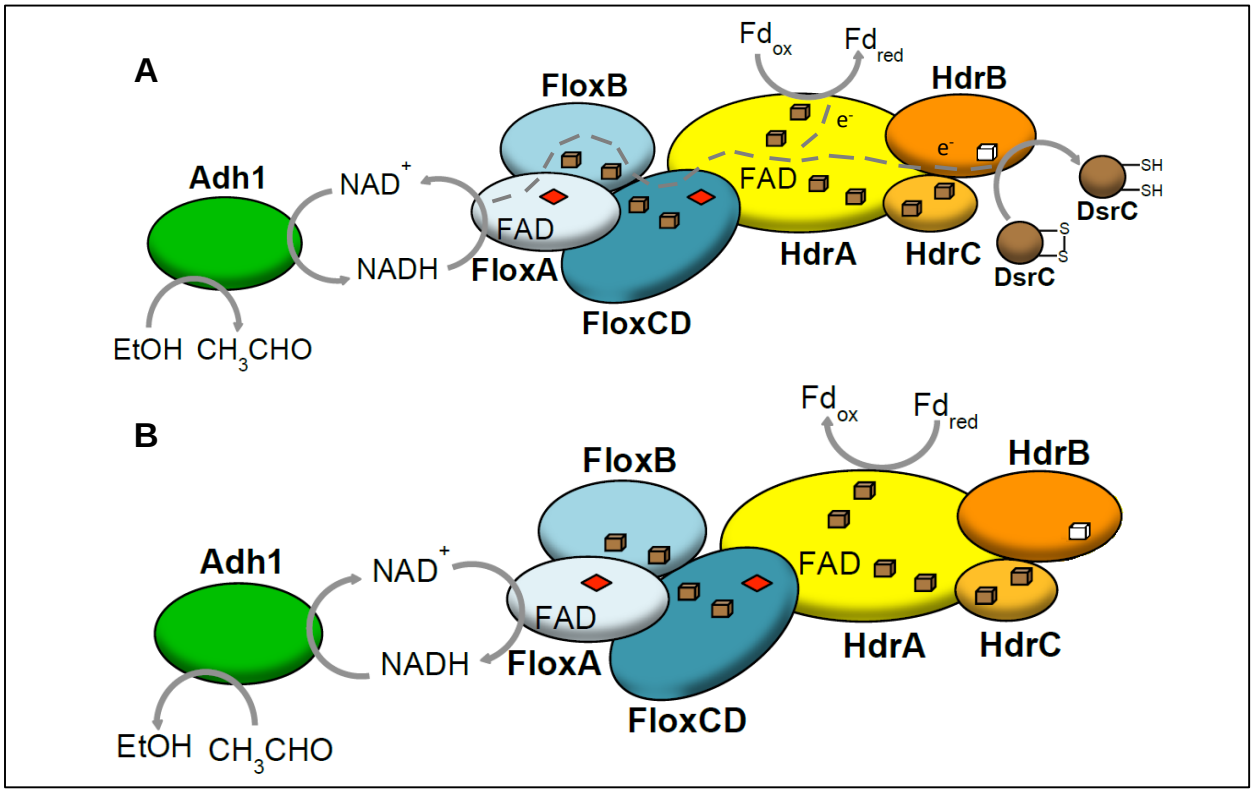

Figure 5.1 – **Mechanism for the function of the HdrABC/FloxABCD complex.** In DvH growing on ethanol-sulfate (**A**), Adh1 oxidizes ethanol (EtOH) producing NADH. This product is than oxidized by FloxABCD and the electrons are transferred to HdrABC, which can then bifurcate to the reduction of Fdx and DsrC. In pyruvate fermentation conditions (**B**) the Flox-Hdr complex functions in the opposite direction, but without the influence of DsrC. Fd_{ox} – Ferredoxin Oxidized form, Fd_{red} – Ferredoxin reduced form. Adapted from (58).

Further studies should be performed to search for other possible physiological partners of DsrC. The proteins that were pulled down with DsrC and analysed by mass spectrometry did not reveal the presence of Ldh1a, Ldh1b, LldEFG, Ldh3 or HdrG co-eluting with DsrC during lactate oxidation. However, this does not mean that those proteins are not acting as partners of DsrC. So, further studies should be performed using a more sensitive method like Western blot and use specific antibodies against those proteins. Additionally, the transmembrane complexes DsrMKJOP, HmcABCDEF and TmcABCD that are proposed to reduce DsrC during sulfite reduction should also be analysed. To achieve this goal the same strategies as the ones

performed here using mass spectrometry and Western blot could be performed using the membrane fractions obtained by pull down assays in order to identify the membrane-bound complexes that are electron partners of DsrC.

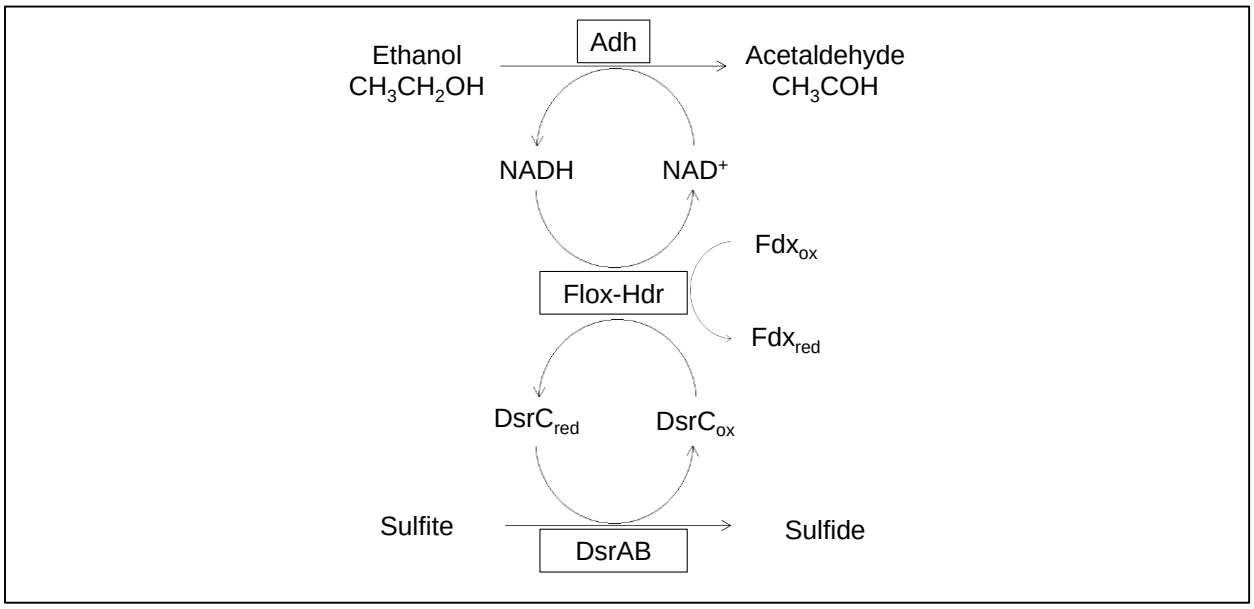

Figure 5.2 – **DsrC as a link between dissimilatory sulfite reduction and ethanol oxidation pathways.** Fd_{ox} - Ferredoxin oxidized form, Fd_{red} – Ferredoxin reduced form, $DsrC_{ox}$ – DsrC oxidized form, $DsrC_{red}$ – DsrC reduced form.

References

1. J. Nicholson, E. Holmes, J. Kinross, R. Burcelin, G. Gibson, W. Jia, S. Pettersson, Host-gut microbiota metabolic interactions, *Science* **336**, 1262 (2012).
2. C. Lozupone, J. Stombaugh, J. Gordon, J. Jansson, R. Knight, Diversity, stability and resilience of the human gut microbiota, *Nature* **489**, 220 (2012).
3. L. Hooper, D. Littman, A. Macpherson, Interactions between the microbiota and the immune system, *Science* **336**, 6086 (2012).
4. F.Sommer, F. Bäckhed, The gut microbiota - masters of host development and physiology, *Nature reviews. Microbiology* **11**, 227 (2013).
5. F. Fava, S. Danese, Intestinal microbiota in inflammatory bowel disease: friend of foe?, *World Journal of Gastroenterology* **17**, 557 (2011).
6. J. Cho, The genetics and immunopathogenesis of inflammatory bowel diseases, *Nature reviews. Immunology* **8,** 458 (2008).
7. J. Jin, Inflammatory Bowel Disease, *The Journal of the American Medical Association* **311**, 2034 (2014)
8. R. Sartor, Mechanisms of disease: pathogenesis of Crohn's disease and ulcerative colitis, *Nature Clinical Practice. Gastroenterology & Hepatology* **3**, 390, (2012).
9. V. Zinkevich, I. Beech, Screening of sulfate-reducing bacteria in colonoscopy samples from healthy and colitic human gut mucosa, *FEMS Microbiology Ecology* **34**, 147 (2000).
10. A. Fite, G. Macfarlane, J. Cummings, M. Hopkins, S. Kong, E. Furrie, S. Macfarlane, Identification and quantitation of mucosal and faecal *desulfovibrios* using real time polymerase chain reaction, *Gut* **53**, 523 (2004).
11. F. Carbonero, A. Benefiel, H. Gaskins, Contributions of the microbial hydrogen economy to colonic homeostasis, *Nature Reviews. Gastroenterology & Hepatology* **9**, 504 (2012).
12. G. Gibson, J. Cummings, G. Marfarlane, Growth and activities of sulphate-reducing bacteria in gut contents of healthy subjects and patients with ulcerative colitis, *FEMS Microbiology Ecology* **86**, 103 (1991).
13. G. Gibson, T. Macfarlane, J. Cummings, Occurrence of sulphate-reducing bacteria in human faeces and the relationship of dissimilatory sulphate reduction to methanogenesis in the large gut, *Journal of Applied Bacteriology* **65**, 103 (1988).
14. F. Rey, M. Gonzalez, J. Cheng, M. Wu, P. Ahern, J. Gordon, Metabolic niche of a prominent sulfate-reducing human gut bacterium, *Proceedings of the National Academy of Sciences* **110,** 13582 (2013).
15. J. Loubinoux, J. Bronowicki, I. Pereira, J. Mougenel, A. Faou, Sulfate-reducing bacteria in human feces and their association with inflammatory bowel diseases, *FEMS Microbiology Ecology* **40**, 107 (2002).
16. M. Ramos, E. Wagner, M. Plewa, H. Gaskins, Evidence that hydrogen sulfide is a genotoxic agent, Molecular Cancer Research **4**, 9 (2006).
17. R. Sartor, Microbial Influences in Inflammatory Bowel Diseases, *Gastroenterology* **134**, 577 (2008).
18. S. Zeissig, N. Burgel, D. Gunzel, J. Richter, J. Mankertz, U. Wahnschaffe, A. Kroesen, M. Zeitz, M. Fromm, J. Schulzke, Changes in expression and distribution of claudin 2, 5 and 8 lead to discontinuous tight junctions and barrier dysfunction in active Crohn's disease, *Gut* **56**, 61 (2007).
19. S. Vetrano, M. Rescigno, M. Cera, C. Correale, C. Rumio, A. Doni, M. Fantini, A. Sturm, E. Borroni, A. Repici, M. Locati, A. Malesci, E. Dejana, S. Danese, Unique role of junctional adhesion molecule-A in maintaining mucosal homeostasis in Inflammatory Bowel Disease, *Gastroenterology* 135, 173 (2008).
20. A. Phalipon, A. Cardona, J. Kraehenbuhl, L. Edelman, P. Sansonetti, B. Corthésy, Secretory component: A new role in secretory IgA-mediated immune exclusion *In Vivo*, *Immunity* **17**, 107 (2002).
21. A. Cerutti, M. Rescigno, The biology of intestinal immunoglobulin A responses, *Immunity* **28**, 740 (2008).

22. M. Bowles, J. Mogollón, S. Kasten, M. Zabel, K. Hinrichs, Global rates of marine sulfate reduction and implications for sub–sea-floor metabolic activities, *Science* **344**, 889 (2014).
23. L. Barton, G. Fauque, Biochemistry, physiology and biotechnology of sulfate-reducing bacteria. *Advances in Applied Microbiology* **68**, 41 (2009).
24. D. Ligthelm, A. Boer, J. Brint, Reservoir souring: an analytical model for H_2S generation and transportation in an oil reservoir owing to bacterial activity, *Society of Petroleum Engineers* **0**, 369 (1991).
25. G. Voordouw, Production-related petroleum microbiology: progress and prospects, *Current opinion in Biotechnology* **11**, 401 (2011).
26. D. Lovley, E. Roden, E. Phillips, J. Woodward, Enzymatic iron and uranium reduction by sulfate-reducing bacteria, *Marine Geology* **113**, 41 (1993).
27. J. Simon, P. M. Kroneck, Microbial sulfite respiration. *Advances in Microbial Physiology* **62**, 45 (2013).
28. G. Muyzer, A. Stams, The ecology and biotechnology of sulphate-reducing bacteria, *Nature reviews. Microbiology* **6**, 441 (2008).
29. R. Rabus, S. Venceslau, L. Wöhlbrand, G. Voordouw, J. Wall, I. Pereira, A post-genomic view of the ecophysiology, catabolism and biotechnological relevance of sulfate-reducing prokaryotes, *Advances in microbial physiology* **66**, 55 (2015).
30. T. Woyke, H. Teeling, N. Ivanova, M. Huntemann, M. Richter, F. Gloeckner, D. Boffelli, I. Anderson, K. Barry, H. Shapiro, E. Szeto, N. Kyrpides, M. Mussmann, R. Amann, C. Bergin, C. Ruehland, E. Rubin N. Dubilier, Symbiosis insights through metagenomic analysis of a microbial consortium, *Nature* **443**, 950 (2006).
31. A. Boetius, K. Ravenschlag, C. Schubert, D. Rickert, F. Widdel, A. Gieseke, R. Amann, B. Jùrgensen, U. Witte O. Pfannkuche, A marine microbial consortium apparently mediating anaerobic oxidation of methane, *Nature* **407**, 623 (2000).
32. R. Rabus, A. Ruepp, T. Frickey, T. Rattei, B. Fartmann, M. Stark, M. Bauer, A. Zibat, T. Lombardot, I. Becker, J. Amann, K. Gellner, H. Teeling, W. D. Leuschner, F. Glöckner, A. Lupas, R. Amann, H. Klenk The genome of *Desulfotalea psychrophila*, a sulfate-reducing bacterium from permanently cold Arctic sediments, *Environmental Microbiology* **6**, 887 (2004).
33. F. Grein, A. Ramos, S. Venceslau, I. Pereira, Unifying concepts in anaerobic respiration: insights from dissimilatory sulfur metabolism, *Biochimica et Biophysica Acta* **1827**, 145 (2013).
34. T. Leustek, M. Martin, J. Bick, J. Davies, Pathways and regulation of sulfur metabolism revealed through molecular and genetic studies, *Annual Review of Plant Physiology and Plant Molecular Biology* **51**, 141 (2000).
35. A. Sass, H. Rütters, H. Cypionka, H. Sass*, Desulfobulbus mediterraneus* sp. nov., a sulfate-reducing bacterium growing on mono- and disaccharides, *Archives of Microbiology* **177**, 468 (2002).
36. A. Stams, T. Hansen G. Skyring, Utilization of amino acids as energy substrates by two marine *Desulfovibrio* strains, *FEMS Microbiology Ecology* **31**, 11 (1985).
37. G. Harms, K. Zengler, R. Rabus, F. Aeckersberg, D. Minz, R. Rosselló-Mora, F. Widdel, Anaerobic oxidation of *o*-xylene, *m*-xylene, and homologous alkylbenzenes by new types of sulfate-seducing bacteria, *Applied and Environmental Microbiology* **65**, 999 (1999).
38. J. Heidelberg, R. Seshadri, S. Haveman, C. Hemme, I. Paulsen, J. Kolonay, J. Eisen, N. Ward, B. Methe, L. Brinkac, S. Daugherty, R. Deboy, R. Dodson, A. Durkin, R. Madupu, W. Nelson, S. Sullivan, D. Fouts, D. Haft, J. Selengut, J. Peterson, T. Davidsen, N. Zafar, L. Zhou, D. Radune, G. Dimitrov, M. Hance, K. Tran, H. Khouri, J. Gill, T. Utterback, T. Feldblyum, J. Wall, G. Voordouw, C. Fraser, The genome sequence of the anaerobic, sulfate-reducing bacterium *Desulfovibrio vulgaris* Hildenborough. *Nature Biotechnology* **22**, 554 (2004).
39. K. Keller, J. Wall, Genetics and molecular biology of the electron flow for sulfate respiration in *Desulfovibrio, Frontiers in Microbiology* **2**, 135 (2011).

40. H. Cypionka, Oxygen respiration by *Desulfovibrio* species, *Annual review of Microbiology* **54,** 827 (2000).
41. I. Pereira, A. Ramos, F. Grein, M. Marques, S. Silva, S. Venceslau, A comparative genomic analysis of energy metabolism in sulfate-reducing bacteria and archaea, *Frontiers in Microbiology* **2**, 69 (2011).
42. H. Cypionka, Solute Transport and Cell Energetics, *Biotechnology Handbooks* **8,** 151 (1995).
43. A. Ramos, K. Keller, J. Wall, I. Pereira, The membrane QmoABC complex interacts directly with the dissimilatory adenosine 5'-phosphosulfate reductase in sulfate-reducing bacteria. *Frontiers in Microbiology* **3**, 137 (2012).
44. G. Zane, H. B. Yen, J. Wall, Effect of the deletion of *qmoABC* and the promoter-distal gene encoding a hypothetical protein on sulfate reduction in *Desulfovibrio vulgaris* Hildenborough. *Applied and Environmental Microbiology* **76**, 5500 (2010).
45. T. Oliveira, C. Vonrhein, P. Matias, S. Venceslau, I. Pereira, M. Archer, The crystal structure of *Desulfovibrio vulgaris* dissimilatory sulfite reductase bound to DsrC provides novel insights into the mechanism of sulfate respiration, *The Journal of Biological Chemistry* **283**, 34141 (2008).
46. R. Schweizer, M. Bruschi, G. Voordouw, Expression of the γ-subunit gene of desulfoviridin-type dissimilatory sulfite reductase and of the α- and β-subunit genes is not coordinately regulated, *European Journal of Biochemistry* **211**, 501 (1993).
47. S. Venceslau, J. Cort, E. Baker, R. Chu, E. Robinson, C. Dahl, L. Saraiva, I. Pereira, Redox states of *Desulfovibrio vulgaris* DsrC, a key protein in dissimilatory sulfite reduction, *Biochemical and Biophysical Research Communications* **441**, 732 (2013).
48. D. Canfield, F. Stewart, B. Thamdrup, L. Brabandere, T. Dalsgaard, E. Delong, N. Revsbech, Osvaldo Ulloa, A cryptic sulfur cycle in oxygen-minimum–zone waters off the chilean coast, *Science* **330**, 1375 (2010).
49. F. Stewart , O. Dmytrenko, E. DeLong , C. Cavanaugh, Metatranscriptomic analysis of sulfur oxidation genes in the endosymbiont of *Solemya velum*, *Frontiers in Microbiology.* **2**, 134 (2011).
50. K. Keller, B. J. Giles, E. Semkiw, I. Porat, S. Brown, J Wall, New model for electron flow for sulfate reduction in *Desulfovibrio alaskensis* G20, *Applied Environmental Microbiology* **80**, 855 (2014).
51. S. Venceslau, Y. Stockdreher, C. Dahl, I. Pereira, The "bacterial heterodisulfide" DsrC is a key protein in dissimilatory sulfur metabolism, *Biochimica et Biophysica Acta* **1837,** 1148 (2014).
52. B. Crane, L. Siegel, E. Getzof, Sulfite reductase structure at 1.6 A: Evolution and catalysis for reduction of inorganic anions, *Science* **270**, 59 (1995).
53. L. Chambers, P. Trudinger, Are Thiosulfate and Trithionate Intermediates in Dissimilatory Sulfate Reduction?, *Journal of Bacteriology* **123,** 36 (1975).
54. R. Hedderich, N. Hamann, M. Bennati, Heterodisulfide reductase from methanogenic archaea: a new catalytic role for an iron-sulfur cluster, *Biological Chemistry* **386**, 961 (2005).
55. R. Pires, S. Venceslau, F. Morais, M. Teixeira, A. Xavier, I. Pereira, Characterization of the *Desulfovibrio desulfuricans* ATCC 27774 DsrMKJOP complex - A membrane-bound redox complex involved in the sulfate respiratory pathway, *Biochemistry* **45**, 249 (2006).
56. F. Grein, I. Pereira, C. Dahl, Biochemical characterization of individual components of the *Allochromatium vinosum* DsrMKJOP transmembrane complex aids understanding of complex function in vivo, *Journal of Bacteriology* **192**, 6369 (2010).
57. S. Haveman, V. Brunelle, J. Voordouw, G. Voordouw, J. Heidelberg, R. Rabus, Gene expression analysis of energy metabolism mutants of *Desulfovibrio vulgaris* Hildenborough indicates an important role for alcohol dehydrogenase, *Journal of Bacteriology* **185**, 4345 (2003).
58. R. Ramos, F. Grein, G. Oliveira, S. Venceslau, K. Keller, J. Wall, I. Pereira. The FlxABCD-HdrABC proteins correspond to a novel NADH dehydrogenase/heterodisulfide reductase widespread in anaerobic bacteria and involved in ethanol metabolism in *Desulfovibrio vulgaris* Hildenborough, *Environmental Microbiology* **17,** 2288 (2015).

59. A. Kaster, J. Moll, K. Parey, R. Thauer, Coupling of ferredoxin and heterodisulfide reduction via electron bifurcation in hydrogenotrophic methanogenic archaea, *Proceedings of the National Academy of Sciences* **108,** 2981 (2011).
60. A. Santos, S. Venceslau, F. Grein, W. Leavitt, C. Dahl, D. Johnston, I. Pereira, A protein trisulfide couples dissimilatory sulfate reduction to energy conservation, submitted
61. S. Dadal, E. Chang, The microbial basis of inflammatory bowel diseases, *The journal of Clinical Investigation* **124**, 4190 (2014).
62. S. Chhabra, M. Joachimiak, C. Petzold, G. Zane, M. Price, S. Reveco, V. Fok, A. Johanson, T. Batth, M. Singer, J. Chandonia, D. Joyner, T. Hazen, A. Arkin, J. Wall, A. Singh, J. Keasling, Towards a rigorous network of protein-protein interactions of the model sulfate reducer *Desulfovibrio vulgaris* Hildenborough, *PLoS ONE* **6**, 21470 (2011).
63. N. Vita, O. Valette, G. Brasseur, S. Lignon, Y. Denis, M. Ansaldi, A. Dolla, L. Pieulle, The primary pathway for lactate oxidation in *Desulfovibrio vulgaris*, *Frontiers in Microbiology* **6**, 606 (2015).